J. Phys. B: At. Mol. Opt. Phys. **23** (1990) 4573–4604. Printed in the UK

The multichannel eikonal theory of electron–helium collisions: I. Excitation of He(1^1S)

E J Mansky and M R Flannery

School of Physics, Georgia Institute of Technology, Atlanta, Georgia 30332-0430, USA

Received 14 May 1990

Abstract. Calculations of the integral and differential cross sections for the electronic excitation of the 2^1L and 3^1L states of helium are reported. The multichannel eikonal theory employing a 10-channel basis set is used. The λ and χ parameters for the 2^1P and 3^1P states at 80 eV are also reported. A number of misprints concerning the original multichannel eikonal theory results of Flannery and McCann have occurred in the literature. These misprints are corrected in this paper. A detailed description of both the theoretical *and* experimental difficulties involved in the determination of the integral cross sections $\sigma_{1^1S\rightarrow 3^1S}$ and $\sigma_{1^1S\rightarrow 3^1D}$ is provided. In addition, a critique of the assumptions made in previous experimental determinations of the differential cross sections (both composite and magnetic sublevel) for the 3^1L states of helium is given. A result of this analysis is that the experimental data on the differential cross sections for the 3^1P state need to be re-interpreted in light of the experimental data of van Linden van den Heuvell *et al.* A principal conclusion of this paper is that the first Born approximation underestimates experimental data in the intermediate energy region for $^1S \rightarrow {}^1D$ transitions, in contrast to the trend seen in $^1S \rightarrow {}^1P$ transitions. The reason for such a reversal in $^1S \rightarrow {}^1D$ transitions can be understood in terms of the direct ($i \rightarrow f$), and indirect ($i \rightarrow n \rightarrow f$, etc) mechanisms which are important in the electronic excitation of the 3^1L states of He. In particular, in this paper the importance of indirect mechanisms in the excitation of the 3^1S and 3^1D is shown, thereby confirming the early results of Chung and Lin and the tentative conclusions of Massey.

1. Introduction

Knowledge of the integral cross sections for the electron impact excitation of helium atoms is essential in the interpretation of the spectra of a wide variety of astrophysical and laboratory systems. While electron excitation cross sections for the $1^1S \rightarrow n^{1,3}L$ transitions in helium have been the subject of a great deal of work, both theoretical and experimental, the corresponding problem of computing accurate, converged cross sections $\sigma_{n,n'}$ for transitions $n^{1,3}L \rightarrow n'^{1,3}L'$ between metastable levels of helium has received much less attention during the past thirty years in spite of their importance in applications. In fact, of the metastable transitions $n^{1,3}L \rightarrow n'^{1,3}L'$, in helium which have been studied, the vast majority have involved excitations within the $n = 2$ manifold (i.e. $\Delta n = 0$ transitions, where $\Delta n = n' - n$). However, cross sections for metastable transitions with $\Delta n \geq 1$ are also important in applications. For example, the integral cross section $\sigma_{2,3}$ is important in primordial nucleosynthesis

0953-4075/90/244573+32$03.50

(Ferland 1986), and in the interpretation of the spectra of Seyfert galaxies (Feldman and MacAlpine 1978), as well as in the stepwise ionization of helium atoms in gaseous discharges.

In addition, the recent measurements of the differential cross sections for the excitation of the 3^3L states of helium made in Kaiserslautern (Müller-Fiedler *et al* 1984), and the integral cross sections measurements performed in Madison (Rall *et al* 1989) have demonstrated that it is now feasible to treat metastable $n^{1,3}L \rightarrow n'^{1,3}L'$ transitions in the laboratory in a much more detailed manner than was possible in the pioneering work of Phelps (1955). Hence, the continuing requirements of a wide range of applications, together with the experimental data of Müller-Fiedler *et al* (1984) and Rall *et al* (1989), are the primary motivations of this work.

This paper (I) will update the multichannel eikonal theory (MET) results of Flannery and McCann (McCann and Flannery 1974, Flannery and McCann 1975a, b), for $e^- +$ He collisions, and extend them to a wider range of energies. In particular in this paper we are concerned with computing integral cross sections for the excitation of the 2^1L and 3^1L states of helium by electron impact on He(1^1S). In II, the corresponding problem of the electronic excitation from He($2^{1,3}$S, $2^{1,3}$P) will be considered. The ultimate goal of this series of papers is to provide a set of accurate, converged inelastic integral cross sections $\sigma_{n,n'}$ for transitions with $\Delta n \leq 2$, over a wide range of incident electron energies from the region where the inelastic integral cross section has a maximum, to the high energy limit (wherein the first Born approximation becomes accurate).

In this paper the present MET results for the electron impact excitation of He(1^1S) are compared with a number of other theoretical models ranging from the early coupled equations solution of Chung and Lin (1968, 1969) to the 19-state R-matrix results of Berrington and Kingston (1987). Additional theoretical results discussed later include the 5-state R-matrix results of Fon *et al* (1980, 1981), the DWPO results of Scott and McDowell (1975, 1976) and the FOMBT results of Chutjian and Thomas (1975). Comparison of the present MET results with the theoretical results previously mentioned is provided in section 3.

A number of misprints concerning the original MET results of Flannery and McCann for excitation from He(1^1S) have occurred in the literature. This has lead to incorrect conclusions being drawn regarding the accuracy of the MET results. In section 2 these misprints are corrected and discussed in detail. In section 3 the updated MET results for the integral and differential cross sections are presented, together with a comparison with available experimental and theoretical results. Section 4 contains the conclusions of the paper. Atomic units are used throughout.

2. Theory

The MET for $e^- +$ He(1^1S) collisions was originally developed by Flannery and McCann, first with a 4-channel basis set (McCann and Flannery 1974), then with a 10-channel basis set (Flannery and McCann 1975a). In the preceding paper (Mansky and Flannery 1990) an overview of the original MET was provided, together with a derivation of the dipole correction required (at large impact parameters ρ) for the case of $e^- + A^*$ collisions. Hence, in this paper only the wavefunctions and energy level structure used to characterize the He target atom require discussion. As in the preceding paper, the present multichannel eikonal results will be denoted DMET to

indicate the addition of the dipole correction at large ρ to the original MET results. In this paper we are interested in the following collision processes,

$$e^- + He(1^1S) \rightarrow e^- + He(1^1S, 2^1S, 2^1P_0, 2^1P_{\pm 1}, 3^1S, 3^1P_0, 3^1P_{\pm 1}, 3^1D_0, 3^1D_{\pm 1}, 3^1D_{\pm 2})$$

where the target He atom is initially in the ground state, and a 10-channel basis set is used. Electron exchange effects are omitted, so that couplings only within the singlet manifold are considered. In the coupled first-order partial differential equations satisfied by the amplitude functions $C_n(\rho, z)$ the interaction matrix elements V_{nj} are defined,

$$V_{nj}(\boldsymbol{R}) = \langle \Psi_n(\boldsymbol{r}_1, \boldsymbol{r}_2) \mid V(\boldsymbol{r}_1, \boldsymbol{r}_2, \boldsymbol{R}) \mid \Psi_j(\boldsymbol{r}_1, \boldsymbol{r}_2) \rangle \tag{1}$$

where the two-electron He wavefunctions $\Psi_n(\boldsymbol{r}_1, \boldsymbol{r}_2)$ are the analytical Hartree–Fock frozen-core wavefunctions of McEachran and coworkers (Cohen and McEachran 1967, McEachran and Cohen 1969, Crothers and McEachran 1970), and are defined as

$$\Psi_{1s,nlm}(\boldsymbol{r}_1, \boldsymbol{r}_2) = N_{nl}[\varphi_{1s}(\boldsymbol{r}_1)\varphi_{nlm}(\boldsymbol{r}_2) + \varphi_{1s}(\boldsymbol{r}_2)\varphi_{nlm}(\boldsymbol{r}_1)]. \tag{2}$$

The normalized eigenfunction representing the frozen 1s core orbital is

$$\varphi_{1s}(\boldsymbol{r}) = 2^{5/2} e^{-2r} Y_{00}(\hat{r})$$

while the unnormalized orbital for the state nlm is given by

$$\varphi_{nlm}(\boldsymbol{r}) = \sum_{j=2l+1}^{N_{max}} a_j^{(nl)} (2r)^l \exp(-\beta r) L_j^{(2l+1)}(2\beta r) Y_{lm}(\hat{r}) \tag{3}$$

where $\beta = 2/n$, and the coefficients $a_j^{(nl)}$ have been tabulated by McEachran and coworkers. In this paper the coefficients $a_j^{(nl)}$ were taken from the work of Crothers and McEachran (1970), with additional terms as communicated by McEachran (1974). The associated Laguerre polynomials $L_j^{(\lambda)}(x)$ in (3) are defined as follows

$$L_j^{(\lambda)}(x) = \sum_{k=0}^{j-\lambda} \frac{(-1)^{k+1}(j!)^2}{k!(j-k-\lambda)!(k+\lambda)!} x^k. \tag{4}$$

It will prove useful in the evaluation of the matrix elements V_{nj} to rearrange the series in (3) as a sum of Slater orbitals:

$$\varphi_{nlm}(\boldsymbol{r}) = \sum_{N=l+1}^{N_{max}-l} B_N^{(nl)} r^{N-1} e^{-\beta r} Y_{lm}(\hat{r}) \tag{5}$$

where the coefficients $B_N^{(nl)}$ are now defined as

$$B_N^{(nl)} = \sum_{j=N+l}^{N_{max}} a_j^{(nl)} \frac{(-1)^{N-l} 2^l (2\beta)^{N-l-1} (j!)^2}{(N-l-1)!(N+l)!(j-N-l)!}. \tag{6}$$

Note that a misprint in the definition of the $B_N^{(nl)}$ coefficients occurs in McCann and Flannery (1974, their equation (30*b*)). The first factorial in the denominator of their equation (30*b*) should be $(N-l-1)!$ instead of $(n-l-1)!$. The correct form was given in their later papers and was used in all three of their calculations. The number of $a_j^{(nl)}$ coefficients used is denoted by $N_{\max}$, and varies between 9 and 11 for the wavefunctions used in this paper. The normalization constant N_{nl} in equation (2) is $(2[H_{nl}+G_{nl}^2])^{-1/2}$, with the functions H_{nl} and G_{nl} given by

$$H_{nl} = \sum_{N=l+1}^{N_{\max}-l} \sum_{N'=l+1}^{N_{\max}-l} B_N^{(nl)} B_{N'}^{(nl)} \frac{(N+N')!}{(2\beta)^{N+N'+1}} \tag{7a}$$

$$G_{nl} = 2^{5/2}\delta_{l0} \sum_{N=l+1}^{N_{\max}-l} B_N^{(nl)} \frac{(N+1)!}{(\beta+2)^{N+2}}. \tag{7b}$$

It should also be noted that a misprint in the tabulation of the $B_N^{(nl)}$ coefficients occurs in McCann and Flannery (1974). The $B_N^{(nl)}$ coefficients given in their table 1 are actually the product $N_{nl} \cdot B_N^{(nl)}$. The normalization constants N_{nl} tabulated by McCann and Flannery (1974) in their table 1 are correct. In addition, the correct values of the $B_N^{(nl)}$ coefficients (as given by (5)) were used by Flannery and McCann in all three of their $e^- + He$ calculations, so the misprint is not a serious one. However, for completeness, the correct $B_N^{(nl)}$ coefficients are presented in table 1 for all wavefunctions used in this paper. Also, the normalization constant N_{nl}, and the calculated and observed energies of the eigenstates are given in table 1. The calculated energies of the target states are taken from the work of McEachran and coworkers, while the observed energies are taken from the tabulation of Bashkin and Stoner (1975). In the calculations reported in this paper, the observed values of Bashkin and Stoner are used for the energies ϵ_n of the target basis states.

A more serious misprint concerning the original MET results of Flannery and McCann occurs in part II of the review of Bransden and McDowell (1978). In that review the MET results of Flannery and McCann (therein labelled MCE) given in tables 3.17, 3.18 and 3.20 *should all be divided by* 2π. The reason for the misprint lies in the computer program used for the original MET calculations. Denoting the differential and integral cross sections for excitation of channel n by $\sigma_n(\theta)$ and σ_n, respectively, the integral cross section σ_n is given by (in units of a_o^2)

$$\sigma_n = \int_0^{2\pi} \mathrm{d}\Phi \int_0^{\pi} \sigma_n(\theta)\sin(\theta)\,\mathrm{d}\theta = 2\pi \int_0^{\pi} \sigma_n(\theta)\sin(\theta)\,\mathrm{d}\theta. \tag{8}$$

It is natural then to tabulate the product $2\pi \cdot \sigma_n(\theta)$, and this is what the computer program used in the original MET calculations printed. Copies of the print-out of the original MET program, containing tabulations of the product $2\pi \cdot \sigma_n(\theta)$, were sent to McDowell during the writing of the review (cf p 292 of Bransden and McDowell 1978). Unfortunately the factor of 2π was not divided-out of the tabulated MET values in the preparation of tables 3.17, 3.18 and 3.20 for the differential cross sections $\sigma_n(\theta)$, but *was* in the preparation of figures 3.4 and 3.5 in Bransden and McDowell (1978). The tabulation of the product $2\pi \cdot \sigma_n(\theta)$ instead of $\sigma_n(\theta)$ in the review of Bransden and McDowell (1978) (cf pp 295–7 and 305) leads them to conclude that the original

Table 1. Slater orbital coefficients $B_N^{(nl)}$ defining the helium wavefunctions used in this paper. 1 atomic unit of energy (au) = 27.2 eV.

	nl					
N	1s	2s	2p	3s	3p	3d
1	−8.0833, −1	−6.0952		2.0653, +1		
2	1.2863, −2	6.0784	−3.9130	−2.4657, +1	−1.0965, +1	
3	−5.4217, −1	−5.3910	−7.6800, −2	1.7354, +1	1.6439	−8.8743, +1
4	−2.0726, −3	4.5264	−2.5896	−1.1852, +1	−4.5108	−1.4563, +1
5	4.7345, −2	−1.6637	1.0664	4.3143	2.5759	−1.8768, +1
6	−3.5140, −2	4.2289, −1	−3.7921, −1	−9.4909, −1	−8.4067, −1	6.3070
7	8.9689, −3	−6.3609, −2	7.0036, −2	1.3332, −1	1.7956, −1	−1.9705
8	−1.1540, −3	5.9499, −3	−8.2660, −3	−1.1648, −2	−2.4862, −2	3.3455, −1
9	5.4661, −5	−3.0144, −4	5.1189, −4	6.2566, −4	2.3062, −3	−3.7988, −2
10		6.9148, −6	−1.4916, −5	−1.8610, −5	−1.3983, −4	2.7044, −3
11				2.4687, −7	5.3777, −6	−1.2085, −4
12					−1.1841, −7	3.0321, −6
13					1.1773, −9	−3.4580, −8
N_{nl}	2.2745	9.1921, −2	3.6218, −2	1.4286, −2	7.4796, −3	7.4551, −5
ϵ (au)[a]	0.87251	0.14344	0.12245	0.06057	0.05474	0.05555
ϵ (au)[b]	0.90357	0.14596	0.12383	0.06127	0.05514	0.05562

[a] Theoretical energies from McEachran and co-workers (see references).
[b] Experimental energies from Bashkin and Stoner (1975).

MET results for $\sigma_{2^1S}(\theta)$ and $\sigma_{3^1S}(\theta)$ were at variance with and much higher (by $\sim 2\pi$) than a number of other theoretical results. In section 3.2 of this paper tables 3, 4, 5 and 7 are given which correct and replace tables 3.17, 3.18 and 3.20 of Bransden and McDowell (1978). The conclusions drawn by Bransden and McDowell, regarding the original MET results of Flannery and McCann, are similarly updated in section 3.2 of this paper.

The two key differences between the current calculations and the original MET results of Flannery and McCann (1975a) are the improved numerical solution of the coupled equations satisfied by the $C_n(\rho, z)$, and the inclusion (for large $\rho \geq \rho_{\max}$) of the dipole correction to the scattering amplitude $f_{ni}(\theta)$. The details of the numerical solution of the coupled equations will be given elsewhere (Mansky 1990a), while the derivation of the dipole correction is presented in the preceding paper (Mansky and Flannery 1990). The principal advantage of the improved numerical solution of the coupled equations is to extend the energy range considered down to 24 eV from the original lower limit of 40 eV. While the dipole correction to the $f_{ni}(\theta)$ will be most pronounced in the integral cross sections for dipole-coupled transtions in $e^- + A^*$ collisions, it cannot be neglected in the differential cross sections for $1^1S \rightarrow n'^1P$ transitions in $e^- + A$ collisions—especially in the forward direction at high energies.

The two main assumptions made in this paper and in the original MET results of Flannery and McCann for $e^- + He(1^1S)$ collisions are that the trajectory characterizing the relative motion of the electron is well approximated by a straight-line, and that the influence of electron exchange on the inelastic integral cross sections will be small since exchange is important only at larger scattering angles. While the assumption of straight-line trajectories should be accurate in $e^- + He^*$ collisions, due to the dominance of long-range interactions, it can easily be removed and account taken of

the curvature of the trajectory of the electron. This has been done by McCann and Flannery (1975, 1978) for the MET within the context of ion–molecule heavy particle scattering.

However, it is well known that electron exchange effects must be included in order to obtain accurate elastic integral cross sections over a wide range of energies, as well as, inelastic cross sections in the threshold energy region. But, on the other hand, serious discrepancies have been noted (Berrington and Kingston 1987) between theoretical and experimental results for the integral cross sections for the excitation of the $3^3S, 3^1S, 3^3P, 3^3D, 3^1D$ and the 3^1P states at $E = 29.20$ eV. Differences between theoretical (distorted-wave) results and experimental data for the Stokes parameters for the 3^3D state (Donnelly and Crowe 1988), and the angular correlation parameters for the 3^3P state (Donnelly *et al* 1988) have also been observed. These difficulties indicate that a careful analysis of *both* the direct *and* exchange contributions to the cross sections for the excitation of the $n = 3$ manifold of states in the intermediate energy region is necessary in order to understand the errors inherent in the approximations made by the different scattering theories. Analysis of the direct and exchange contributions will be important both in *primary*, or direct, mechanisms of excitation (i.e. transitions which involve only the initial and final states), and in *secondary*, or indirect, mechanisms of excitation (i.e. transitions which involve the initial and final state together with one (or more) intermediate states). In this light then, the present MET results (without electron exchange) will prove useful in the analysis of the direct contribution to the excitation cross sections $\sigma_{n,n'}$, especially for optically forbidden transitions with $\Delta n = 2$.

3. Results and discussion

3.1. Integral cross sections

The DMET integral cross sections for the electron impact excitation of $He(1^1S)$ are shown in figure 1 and table 2 for energies in the range $24 \leq E(\text{eV}) \leq 2000$. Note that the choice of incident energies used in table 2 was governed by the variation of the inelastic integral cross sections $\sigma_{1^1S \to 3^1L}$ for the excitation of the 3^1L states of He in the intermediate energy region ($E \leq 50$ eV). An expanded view of the region from threshold to 100 eV is given in figure 2 of the inelastic integral cross sections of primary interest in this paper. In the case of the $2^1S, 2^1P, 3^1S$ and 3^1P states, the DMET results have converged to within 7% (or better) to the Born results of Bell *et al* (1969) for $E \geq 1000$ eV. In the case of the $\sigma_{1^1S \to 3^1D}$ however, the DMET results have converged only to within about 10% of the Born result of Bell *et al* for $E \geq 500$ eV. And, since the Born version of the MET yields the Born-wave approximation and agrees with the Born results of Bell *et al* , the above convergence rates illustrates the influence that intermediate couplings have on the $\sigma_{1^1S \to n^1L}$ inelastic integral cross sections.

In the case of the $\sigma_{1^1S \to 1^1S}$ elastic cross section, the DMET results converge to within 6% or less of the Born result for $E \geq 2000$ eV. That is, the DMET results significantly underestimates the experimental data (Jansen 1975, as cited by Bransden and McDowell 1978) as expected due to the neglect of full polarization distortion and electron exchange in the present calculations. An indication of the importance of polarization potential effects and electron exchange in the elastic channels is obtained by comparing the 3-state ($1^1S, 2^1S, 2^1P$) close-coupling calculations of Willis *et al*

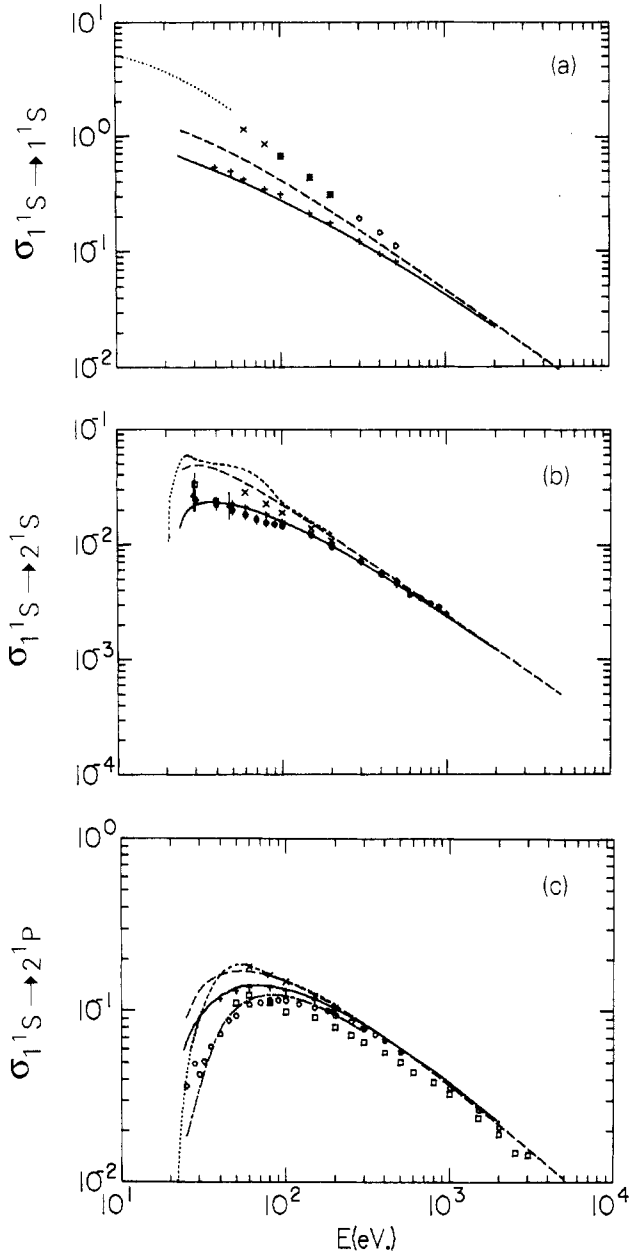

Figure 1. (*a*)–(*c*) Integral cross sections: (*a*) $\sigma_{1^1S\to1^1S}$, (*b*) $\sigma_{1^1S\to2^1S}$ and (*c*) $\sigma_{1^1S\to2^1P}$ (all in πa_0^2) against E (eV). Long broken curve, first Born results (Bell *et al* 1969); full curve, present DMET results; +, original MET results (Flannery and McCann 1975a); ×, Willis *et al* (1981); short broken curve, 5-state R-matrix (Fon *et al* 1980); chain curve, DWPO-II (Scott and McDowell 1976). In (*a*): dotted curve, McEachran and Stauffer (1983); ○, experimental data (Jansen 1975). In (*b*): dotted curve, Fon *et al* (1980); ○, experimental data (de Heer and Jansen 1977); □, experimental data (Trajmar 1973); △, experimental data (Hall *et al* 1973). In (*c*): ○, experimental data (Westerveld *et al* 1979); □, experimental data (Moussa *et al* 1969).

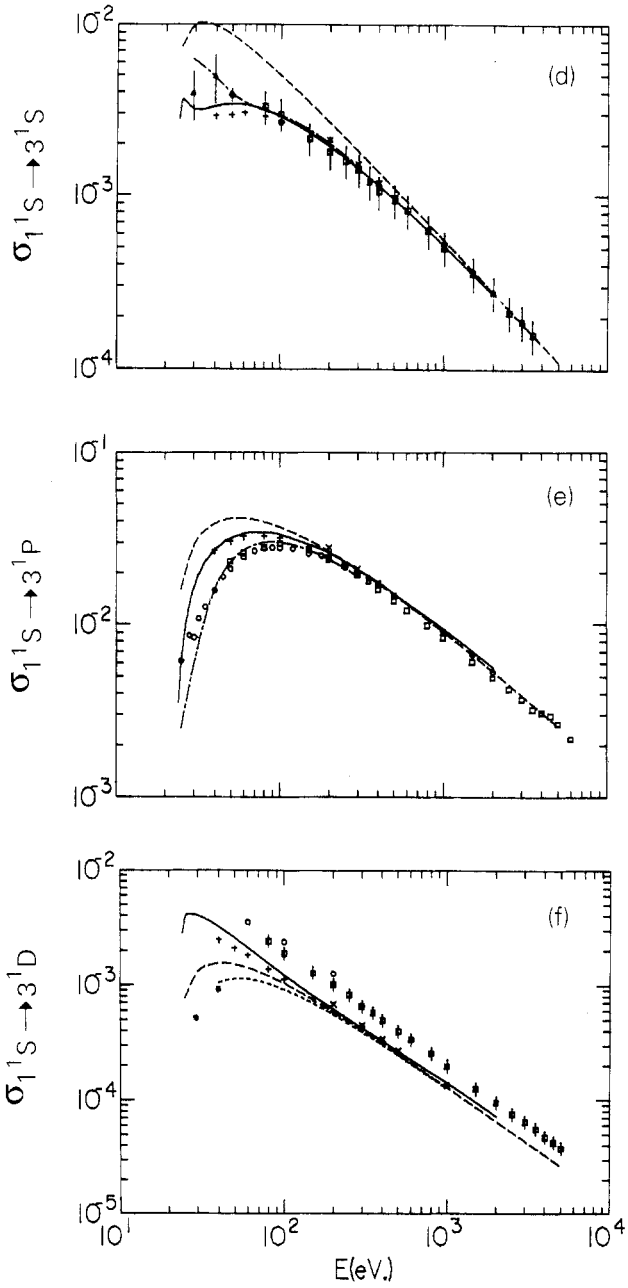

Figure 1. (*d*)-(*f*) Integral cross sections: (*d*) $\sigma_{1^1S\rightarrow3^1S}$, (*e*) $\sigma_{1^1S\rightarrow3^1P}$ and (*f*) $\sigma_{1^1S\rightarrow3^1D}$ (all in πa_0^2) against E (eV). All symbols are the same as figures 1(*a*)-(*c*) except where noted. In (*d*): chain curve, DWPO-I (Scott and McDowell 1975); ×, Bransden and Issa (1975); O, experimental data (van Zyl *et al* 1980); Δ, experimental data (Chutjian and Thomas 1975). In (*e*): ×, Bransden and Issa (1975). In (*f*): short broken curve, Glauber theory (Chan and Chang 1975); *, FOMBT (Chutjian and Thomas 1975); O, experimental data (St John *et al* 1964); Δ, experimental data at 300 eV (Showalter and Kay 1975).

Table 2. DMET integral cross sections $\sigma_{1^1S\to n^1L}(\pi a_0^2)$.

	n^1L					
E (eV)	1^1S	2^1S	2^1P	3^1S	3^1P	3^1D
24	6.77, −1[a]	1.41, −2	5.91, −2	2.78, −3	3.53, −3	2.81, −3
25	6.60, −1	1.66, −2	6.67, −2	3.57, −3	6.23, −3	3.89, −3
26	6.44, −1	1.85, −2	7.23, −2	3.54, −3	8.63, −3	4.08, −3
26.50	6.37, −1	1.92, −2	7.48, −2	3.49, −3	9.75, −3	4.09, −3
27	6.30, −1	1.98, −2	7.84, −2	3.41, −3	1.08, −2	4.12, −3
28	6.16, −1	2.08, −2	8.34, −2	3.28, −3	1.30, −2	4.10, −3
28.50	6.10, −1	2.11, −2	8.48, −2	3.24, −3	1.40, −2	4.08, −3
29	6.04, −1	2.15, −2	8.68, −2	3.21, −3	1.49, −2	4.07, −3
30	5.92, −1	2.20, −2	9.27, −2	3.15, −3	1.64, −2	4.01, −3
31.50	5.75, −1	2.26, −2	9.76, −2	3.13, −3	1.90, −2	3.90, −3
32	5.70, −1	2.27, −2	9.88, −2	3.13, −3	1.95, −2	3.86, −3
34	5.50, −1	2.32, −2	1.07, −1	3.16, −3	2.20, −2	3.70, −3
34.50	5.46, −1	2.32, −2	1.08, −1	3.17, −3	2.27, −2	3.66, −3
36	5.32, −1	2.33, −2	1.12, −1	3.20, −3	2.39, −2	3.52, −3
38	5.16, −1	2.34, −2	1.16, −1	3.25, −3	2.55, −2	3.36, −3
40	5.00, −1	2.33, −2	1.22, −1	3.29, −3	2.73, −2	3.21, −3
42	4.86, −1	2.32, −2	1.25, −1	3.32, −3	2.81, −2	3.06, −3
44	4.73, −1	2.30, −2	1.27, −1	3.36, −3	2.92, −2	2.92, −3
45	4.67, −1	2.29, −2	1.28, −1	3.37, −3	2.98, −2	2.86, −3
46	4.60, −1	2.28, −2	1.30, −1	3.38, −3	3.04, −2	2.80, −3
48	4.49, −1	2.25, −2	1.33, −1	3.38, −3	3.10, −2	2.68, −3
50	4.38, −1	2.23, −2	1.35, −1	3.40, −3	3.15, −2	2.57, −3
54.40	4.15, −1	2.17, −2	1.37, −1	3.39, −3	3.28, −2	2.35, −3
60	3.90, −1	2.09, −2	1.40, −1	3.36, −3	3.36, −2	2.12, −3
70	3.53, −1	1.95, −2	1.40, −1	3.26, −3	3.45, −2	1.79, −3
75.60	3.36, −1	1.88, −2	1.40, −1	3.19, −3	3.43, −2	1.65, −3
80	3.23, −1	1.82, −2	1.40, −1	3.14, −3	3.41, −2	1.56, −3
81.20	3.20, −1	1.81, −2	1.40, −1	3.12, −3	3.41, −2	1.54, −3
90	2.98, −1	1.71, −2	1.36, −1	3.00, −3	3.40, −2	1.37, −3
100	2.77, −1	1.60, −2	1.34, −1	2.87, −3	3.33, −2	1.23, −3
150	2.07, −1	1.22, −2	1.17, −1	2.31, −3	2.92, −2	8.15, −4
200	1.66, −1	9.82, −3	1.03, −1	1.92, −3	2.60, −2	6.22, −4
300	1.20, −1	7.06, −3	8.36, −2	1.43, −3	2.07, −2	4.26, −4
400	9.47, −2	5.51, −3	7.02, −2	1.14, −3	1.76, −2	3.28, −4
500	7.85, −2	4.52, −3	6.05, −2	9.46, −4	1.51, −2	2.67, −4
600	6.70, −2	3.83, −3	5.38, −2	8.10, −4	1.33, −2	2.26, −4
700	5.86, −2	3.32, −3	4.89, −2	7.08, −4	1.20, −2	1.96, −4
800	5.20, −2	2.93, −3	4.49, −2	6.29, −4	1.10, −2	1.74, −4
900	4.68, −2	2.63, −3	4.13, −2	5.67, −4	1.02, −2	1.56, −4
1000	4.25, −2	2.38, −3	3.82, −2	5.15, −4	9.48, −3	1.41, −4
2000	2.22, −2	1.22, −3	2.27, −2	2.70, −4	5.67, −3	7.25, −5

[a] $6.77, -1 \equiv 6.77 \times 10^{-1}$.

(1981) and the adiabatic exchange approximation results of McEachran and Stauffer (1983) with the DMET results in figure 1(*a*).

For the case of inelastic collisions however, the inclusion of electron exchange is much more difficult due primarily to the numerical problems of solving large numbers of coupled integro-differential equations. As noted in section 2, recent calculations of Berrington and Kingston (1987) have reported inelastic integral cross section results from a 19-state R-matrix calculation (i.e. involving the solution of the full set

of coupled integro-differential equations including couplings up to the $4^{1,3}F$ level). Although great care was taken to ensure that the theoretical results reported were fully converged for all energies, Berrington and Kingston found significant discrepancies between their R-matrix calculations and the experimental data of Chutjian and Thomas (1975)($3^{1,3}S, 3^3P, 3^3D + 3^1D + 3^1P$), Donaldson *et al* (1972)(3^1P), St John *et al* (1964)($3^3S, 3^3P, 3^3D, 3^1D$) and Westerveld *et al* (1977)(3^1P) for the excitation of the states indicated at an electron energy of 29.20 eV. While additional experimental data is certainly required (especially for the excitation of the triplet manifold from the ground state), further theoretical work is needed to quantify the relative contribution that the direct scattering mechanism compared with the effects of electron exchange has on the integral cross section for the excitation of any particular state in the basis set. Hence theoretical calculations which involve solving the full set of coupled equations both with *and* without electron exchange will be necessary in resolving the theoretical side of the discrepancy at 29.20 eV, and in assessing the accuracy of any approximations used in treating the electron exchange part of the problem. The importance of comparing theoretical calculations (involving the solution of the full set of coupled equations) both with and without electron exchange is well known both in electron–atom collisions and in electron–positive ion collisions (Berrington *et al* 1989).

The DMET results (figure 1(b)) for the 2^1S state are in excellent agreement with the experimental results of de Heer and Jansen (1977) for energies $E \geq 150$ eV and in good overall agreement with the measurements of Trajmar (1973) at 29.60 and 40.1 eV and Hall *et al* (1973) at 29.2, 39.2 and 48.2 eV (figure 2(a)). Only for energies from 50 to 100 eV do the DMET results overestimate the experimental data of de Heer and Jansen. Interestingly, both the 3-state close-coupling results of Willis *et al* (1981) and the 5-state R-matrix calculations of Fon *et al* (1980, 1981) overestimate all the experimental data in figure 1(b) for $E \leq 200$ eV.

However, the DMET results for the $\sigma_{1^1S \rightarrow 2^1P}$ cross section are in agreement with the experimental data of Westerveld *et al* (1979) only for energies $E \geq 200$ eV, and within the error bounds of the one measurement of Shemansky *et al* (1985) at 200 eV. At lower energies, the present results clearly overestimate the experimental data of both Westerveld *et al* and Moussa *et al* (1969). This can be seen more clearly in figure 2(b), where an expanded view of the region from threshold to 100 eV of figure 1(b) is given. In addition to the experimental data of Westerveld *et al* (1979) and Moussa *et al* (1969), figure 2(b) also shows the experimental data of Hall *et al* (1973) and the Bethe–Born $\sigma_{1^1S \rightarrow 2^1P}$ cross section recommended by Shemansky *et al* (1985, their equation (9)).

In contrast to the DMET results, the distorted-wave polarized orbital (DWPO-II) results of Scott and McDowell (1976) for the $\sigma_{1^1S \rightarrow 2^1P}$ cross section are in good agreement with the experimental data from 30 to 100 eV. It appears that neglect of full polarization distortion and electron exchange in the DMET are the main reasons that the DMET overestimates the experimental data for $\sigma_{1^1S \rightarrow 2^1P}$ at lower energies. However, the DWPO-II results of Scott and McDowell (1976) have included the contribution of the polarization potential only in the direct scattering channel, while the exchange contribution is computed within the adiabatic exchange approximation. More importantly, the DWPO model of Scott and McDowell employs an uncoupled representation in computing the direct and exchange contributions to the T-matrix for the transition $1^1S \rightarrow 2^1P$, so that only couplings between the initial and final states are retained. Couplings to other singlet states, as well as couplings to the (exchange dominated) triplet manifold of states are neglected in the DWPO model. At present it is difficult

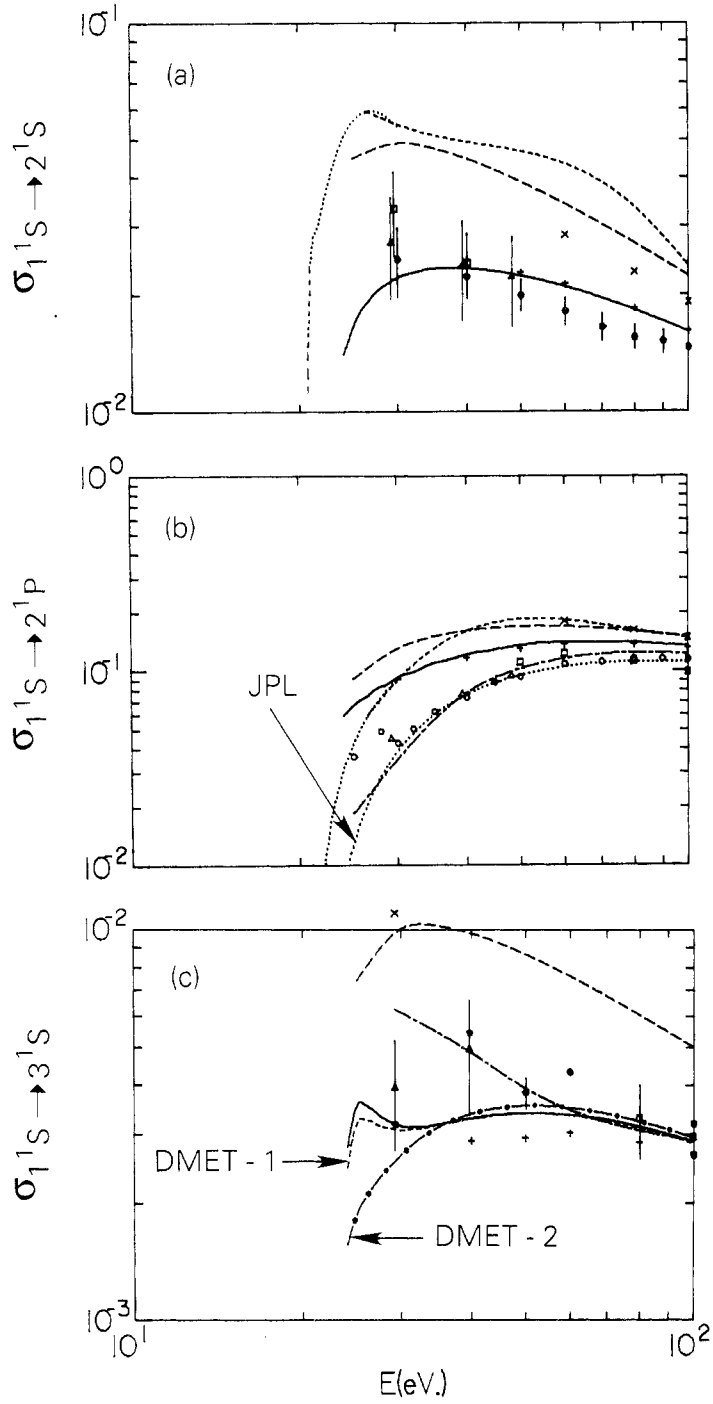

Figure 2. (*a*)–(*c*) Blow-up of figures 1(*b*)–(*d*) from threshold to 100 eV. All symbols are the same as figures 1(*b*)–(*d*) except where noted. In (*b*): JPL, equation (9) of Shemansky *et al* (1985). In (*c*): ×, 19-state *R*-matrix (Berrington and Kingston 1987); *, FOMBT (Chutjian and Thomas 1975); ●, experimental data (St John *et al* 1964).

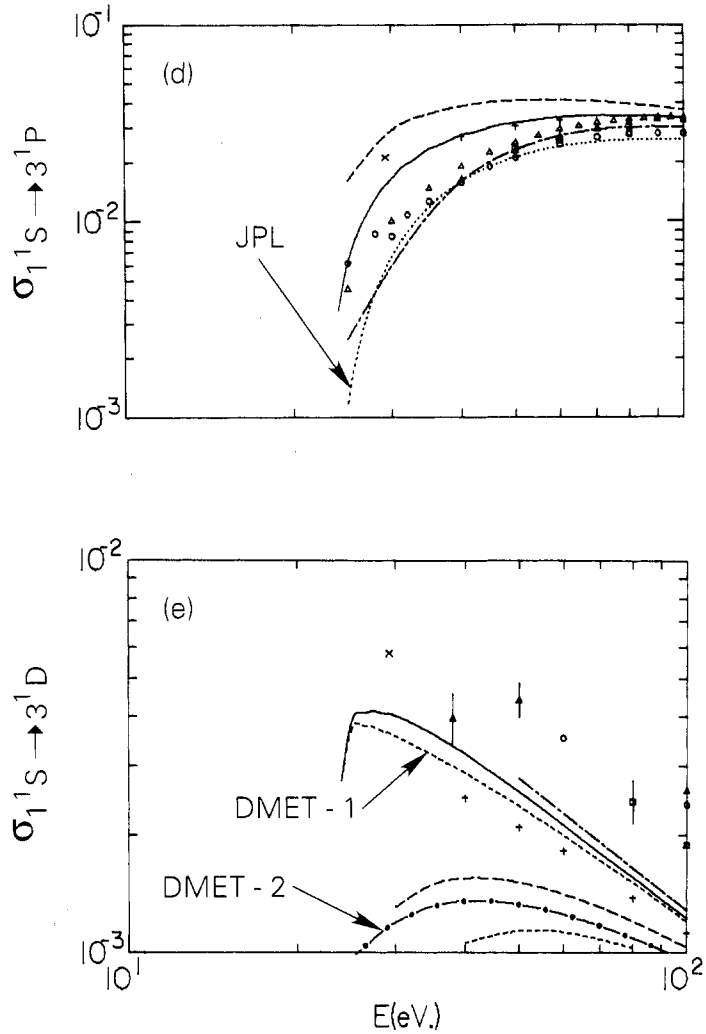

Figure 2. (*d*)–(*e*) Blow-up of figures 1(*e*)–(*f*) from threshold to 100 eV. All symbols are the same as figures 1(*e*)–(*f*) except where noted. ×, 19-state *R*-matrix (Berrington and Kingston 1987); In (*d*): JPL, equation (9) of Shemansky *et al* (1985); △, experimental data (van Raan *et al* 1971, device 1); ▲, experimental data (van Raan *et al* 1971, device 2); short broken curve, *partial* DMET results without quadrupole couplings experimental (see text for details); chain curve, *partial* DMET results without dipole couplings (see text for details). In (*e*): Chain curve, SODM (Baye and Heenen 1974b); △, experimental data (Anderson *et al* 1969).

to assess whether compensating errors have been introduced into the DWPO by the retention of exchange and direct polarization terms and the neglect of couplings to other intermediate states in the case of the $1^1S \rightarrow 2^1P$ transition.

The contribution that couplings to other intermediate states make to inelastic integral cross section can be seen more clearly in the case of the excitation of the 3^1S, 3^1P and 3^1D states of helium. In particular, the DMET results (figures 1(*d*), 2(*c*)) for the excitation of the 3^1S state predicts a double-peak structure to the cross

section. The first peak occurs at an electron energy of 26 eV, with a subsequent flat minimum at 30 eV. The second broader and more familiar peak occurs at 50 eV with a magnitude slightly larger than the first peak. Support for the 26 eV peak in the DMET results for the $\sigma_{1^1S\rightarrow 3^1S}$ cross section comes from two sources. First, a similiar peak (at 25.50 eV) is seen in the 11-state R-matrix results of Berrington *et al* (1985, their figure 3), the magnitude of which however is nearly a factor of five larger than the DMET results. The 11-state R-matrix results also seem to show that the $\sigma_{1^1S\rightarrow 3^1S}$ cross section then declines to a minimum at 30 eV. Unfortunately, the 11-state (Berrington *et al* 1985) and 19-state (Berrington and Kingston 1987) R-matrix results are limited to electron energies $E \leq 30$ and 32 eV, respectively. Hence, while both the R-matrix theory and the DMET predict a maximum in the $\sigma_{1^1S\rightarrow 3^1S}$ at low energies ($E = 25$–26 eV), and a minimum at about 30 eV, it is difficult to understand how inclusion of exchange can result in an increase in the cross section by nearly a factor of five. If subsequent R-matrix and other fully coupled calculations confirm the magnitude of the $\sigma_{1^1S\rightarrow 3^1S}$ cross section at 30 eV and are extended to energies ≥ 30 eV, an important constraint on these calculations will be the benchmark experimental data of van Zyl *et al* (1980)—especially their data point at 50 eV (see figure 2(c)). Hence additional measurements at a finer grid of energies from threshold to 50 eV would be welcomed. Further measurements of the differential and integral cross sections for the excitation of the $3^{1,3}L$ states would then allow a discrimination to be made between the DMET results and the DWPO-I results of Scott and McDowell (1975) for the $\sigma_{1^1S\rightarrow 3^1S}$ cross section at 40 eV.

Secondly, it is interesting to note that in the experimental data of van den Bos *et al* (1968) on the proton excitation of He, that their results for the $\sigma_{1^1S\rightarrow 4^1S}$ inelastic integral cross section exhibits a low energy peak similar to the one observed in the excitation of the 3^1S state in the electron–helium case above. In the case of proton–helium collisions, the low energy peak in the $\sigma_{1^1S\rightarrow 4^1S}$ cross section is a result of the complicated interplay between the many strong interchannel couplings present among the $n = 2, 3, 4$ manifold of states in He, together with the onset of the charge-transfer rearrangement channel at low energies.

The absolute cross section measurements of Moussa *et al* (1969) and van den Bos *et al* (1968) both employed an optical monochromator which was calibrated by means of a standard tungsten ribbon lamp. In the electron–helium measurements of Moussa *et al* the standard deviation of the systematic errors was 7.4% for transitions whose wavelengths λ are between 3000 and 6000 Å. At longer wavelengths $\lambda > 6000$ Å, Moussa *et al* state that the error will be larger. In fact, in the measurement of the cross sections for the 3^1S and 3^1D states of He, the intensity of the radiation emitted in the decays $3^1\text{S} \rightarrow 2^1\text{P}$ and $3^1\text{D} \rightarrow 2^1\text{P}$ is detected. This radiation occurs at wavelengths of 7281 and 6678 Å, for the 3^1S and 3^1D states, respectively. As discussed in detail by van den Bos *et al* (1968), operation of the monochromator at these wavelengths resulted in additional errors of 20% and 10%, respectively, due to the influence of stray light and lowered efficiency of the monochromator. Therefore, in this paper the experimental data of Moussa *et al* for the excitation of the 3^1S state (figures 1(d) and 2(c)) and 3^1D state (figures 1(f) and 2(e)) are shown with error bars of 21.3% and 12.4%, respectively, and which are the square roots of the sum of the squares of the standard deviation of the systematic and additional errors present in these two cases. In this way a rough idea is obtained of the difficulty of the measurements in these cases. Clearly further experimental data would be welcome—especially along the lines of the benchmark measurements of van Zyl *et al* (1980) for both the 3^1S state

(for energies from threshold to 50 eV), and the 3^1D state (from threshold to 1 keV).

Regarding the DMET results for the $\sigma_{1^1S\rightarrow 3^1P}$ little needs to be said since much of the discussion relating to the excitation of the 2^1P state also pertains to the 3^1P state. We simply note that the DMET results for the $\sigma_{1^1S\rightarrow 3^1P}$ integral cross section overestimates the experimental data of Westerveld *et al* (1979) and the Bethe–Born cross section of Shemansky *et al* (1985) for energies $E \leq 100$ eV. The DMET results are, however, in agreement with the experimental data of van Raan *et al* (1971) down to an incident electron energy of 70 eV, below which they then overestimate the measurements. Note that the agreement between the DMET results and the measurements of Westerveld *et al* and van Raan *et al* at their lowest energies is clearly fortuitous.

The principal feature of the DMET results for the $\sigma_{1^1S\rightarrow 3^1D}$ cross section is that a peak occurs (at 28 eV) which is about a factor of three *higher* than the first Born results of Bell *et al* (1969) in the intermediate energy region. Also, we note that convergence to the Born results of Bell *et al* at high energy is much slower in the case of the 3^1D state than in the other inelastic transitions studied in this paper. While no experimental data on the $\sigma_{1^1S\rightarrow 3^1D}$ cross section exists for $E \leq 38$ eV the measurements of Moussa *et al* (1969), St John *et al* (1964), Anderson *et al* (1969) and Showalter and Kay (1975) all show that the experimental results for the $\sigma_{1^1S\rightarrow 3^1D}$ cross section are significantly larger than the Born results of Bell *et al* for energies $E \leq 1$ keV. At higher energies the experimental data of Moussa *et al* for the 3^1D state fails to converge to the Born results of Bell *et al* even at energies as great as 5 keV. While it cannot be ruled out that measurement will converge to the Born result for $E > 5$ keV (say in the 10–50 keV range), in light of the experimental difficulties associated with the operation of the monochromator in the spectral region around 6678 Å, the existence of additional systematic errors left unaccounted for in the experimental data of Moussa *et al* is also a possibility. Clearly, further experimental work on the $\sigma_{1^1S\rightarrow 3^1D}$ cross section at high energies is needed, with emphasis on the absolute calibration of the quantum yield $k(\lambda)$ of the monochromator in the spectral range 6600–7200 Å. In the intermediate energy region the DMET results eventually become larger than the Born result, finally exceeding it by slightly more than a factor of five for $E \leq 30$ eV. This is in qualitative accord with the experimental results shown in figures 1(*f*) and 2(*e*) and is reminiscent of the situation in electron–hydrogen collisions (Mansky and Flannery 1990, preceding paper), wherein the low energy peak of the DMET results for the $\sigma_{1s\rightarrow 3d}$ exceeds the hydrogenic Born results by a factor of 1.29 .

The first quantitative explanation of the reason why the Born results for the $\sigma_{1^1S\rightarrow 3^1D}$ underestimates the experimental data was given by Vriens (1967), who attributed it to the interference between the direct and exchange scattering mechanisms present in this case. In coming to his conclusions, Vriens relied upon exchange amplitudes computed using Ochkur's approximation. The first explanation involving the solution of the full set of coupled equations was given by Chung and Lin (1968, 1969) (see also the discussion of St John *et al* 1964). In solving the closely-coupled equations, Chung and Lin found that the integral cross section for optically forbidden transitions $1^1S \rightarrow n^1S$, $1^1S \rightarrow n^1D (n = 3, 4)$ and $1^1S \rightarrow 4^1F$ depended strongly upon the type and number of couplings to intermediate states retained in the close-coupling expansion. Unfortunately, Chung and Lin only presented detailed results at an electron energy of 100 eV, so a general comparison with the DMET results for energies $E \leq 100$ eV is difficult.

Therefore, to investigate this point further, we have included in figure 2(*e*), not only the DMET results (hereafter denoted *full* DMET), but the results of two *partial*

DMET calculations. In the first *partial* DMET calculation, the coupled equations for the $C_n(\rho, z)$ are solved with the *quadrupole* couplings $3^1S \rightarrow 3^1D_m$ arbitrarily set equal to zero, while in the second *partial* DMET calculation the *dipole* couplings $2^1P_m \rightarrow 3^1D_{m'}$ and $3^1P_m \rightarrow 3^1D_{m'}$ have been set equal to zero. In this way a rough idea of the importance of the dipole and quadrupole transitions which couple the 3^1D state to the rest of the basis set used in this paper is obtained. It would seem apparent from figure 2(*e*) that the indirect mechanism of exciting the 3^1D state, via couplings to other intermediate states, is the dominant one, thereby confirming the early work of Chung and Lin, and the tentative conclusions of Massey *et al* (1969, 1974). Therefore, while the explanation of Vriens (1967) is, in principle, correct, subsequent experimental work (van Rann *et al* 1974) has shown that the use of Ochkur's approximation can result in theory underestimating measurements by up to an order of magnitude. Also, it is not suprising to find that the $\sigma_{1^1S\rightarrow 3^1D}$ cross section results of the first-order many-body theory (FOMBT) of Chutjian and Thomas (1975) falls significantly below the *full* DMET results. Specifically, the *full* DMET results for the $\sigma_{1^1S\rightarrow 3^1D}$ are greater than the FOMBT results of Chutjian and Thomas at 29.2 and 39.70 eV by factors of 7.78 and 3.49, respectively. In contrast, the *full* DMET results at 100 eV are a factor of 1.19 larger than the Born results of Bell *et al* (1969), while the corresponding results of Chung and Lin are a factor of 3.5 larger than the Born values of Bell *et al*.

Another indication of the importance that couplings to other intermediate states make to the $\sigma_{1^1S\rightarrow 3^1D}$ cross section is obtained by comparing the DMET results with the second-order diagonalization method (SODM) results of Baye and Heenen (1974b). While the SODM results of Baye and Heenen (1974b) and the DMET results in the He case are nearly identical, in the case of $e^- + H(1s \rightarrow 3d)$ collisions it was found (Mansky and Flannery 1990) that the DMET and SODM results (Baye and Heenen 1974a) differed by up to 20% at 50 eV. The reason for the differing relationship between the DMET and SODM results for hydrogen and helium is the omission of the 4^1F_m states in the 22-state basis set used by Baye and Heenen (1974b) in the case of He. They used instead the $5^1S, 5^1P_m$ and 5^1D_m states of He, whereas in the case of H all states up to and including the $4f_3$ were included in the calculation (Baye and Heenen 1974a). Now, experimentally it has been known for many years (Anderson *et al* 1969, van Raan and van Eck 1973, van Raan *et al* 1974, Kay and Simpson 1988) that the $4^{1,3}F$ states play an important role in the cascade contribution to the $3^{1,3}D$ states from higher lying levels. Therefore, theoretical calculations of the integral cross section for the excitation of the 3^1D state of He needs to account for the influence that the strong dipole couplings $3^{1,3}D \rightarrow 4^{1,3}F$ have on the $\sigma_{1^1S\rightarrow 3^1D}$. Because of the omission of the 4^1F_m states in the SODM calculations, it is not suprising (in retrospect) to find that the 10-channel DMET and 22-state SODM results are nearly identical since the extra $\Delta n = 2$ transitions included in the SODM calculations are much weaker than the dipole couplings which were omitted in this case. It is also interesting to note that in this case the 19-state *R*-matrix result of Berrington and Kingston (1987) at 29.20 eV, which does include couplings to the $4^{1,3}F$ states, is a factor of 1.42 greater than the DMET results for $\sigma_{1^1S\rightarrow 3^1D}$.

To conclude our discussion of the DMET inelastic integral cross sections, two interim conclusions are in order. First, while the DMET results for the optically allowed transitions are in good agreement with experiment and the Born results at high energy, the overestimation of the DMET results, when compared with the experimental data for $E \leq 100$ eV is not suprising. This is because of the neglect of electron exchange and polarization distortion effects in the DMET results. However, inclusion of

exchange effects in a theoretical calculation does not necessarily mean that all discrepancies with experiment will be eliminated. For example, while the DMET results for the $\sigma_{1^1S\rightarrow 3^1P}$ cross section at 29 eV overestimates the corresponding Bethe–Born fit of Shemansky *et al* by a factor of 2.7 (see figure 2(*d*)), the 19-state *R*-matrix result of Berrington and Kingston lies a factor of 3.8 above the Bethe–Born cross section of Shemansky *et al*. Hence, we agree with Berrington and Kingston and conclude that remaining discrepancies between theory and experiment previously noted should be taken seriously by both experimentalists and theorists. It is noted that the overestimation of the experimental data by the DMET for the optically allowed transitions is not due to the dipole correction, since the difference between the results with and without the correction is $\leq 0.10\%$ for all $E \leq 100$ eV, and less than 1% for energies ≤ 2 keV.

Our second conclusion is that the integral cross sections for optically forbidden transitions are much more sensitive to the number and types of couplings included in the coupled equations than are the optically allowed transitions. Generally, we find that it is best to include couplings between all states in a basis set since it is difficult to *a priori* determine what the dominant pathways of excitation of a given state will be. The agreement between the DMET results and experiment, for the $\sigma_{1^1S\rightarrow 2^1S}$, $\sigma_{1^1S\rightarrow 3^1S}$ and $\sigma_{1^1S\rightarrow 3^1D}$ cross sections overall is quite good. It would seem apparent from figures 2(*c*) and (*e*) that distorted-wave theories have an increasingly difficult time accurately predicting inelastic integral cross sections for optically forbidden transitions when $\Delta \geq 2$ and $\Delta l \geq 1$. Interestingly, the original MET results of Flannery and McCann (1974) differs noticeably from the DMET results only for $\sigma_{1^1S\rightarrow 3^1S}$ and $\sigma_{1^1S\rightarrow 3^1D}$ for $E \leq 100$ eV, and is a direct consequence of the improved numerical solution of the coupled equations in the present calculation (Mansky 1990a).

3.2. Differential cross sections

An overview of the DMET differential cross section (DCS) results at a selection of scattering angles and energies is provided by figure 3. A more detailed tabulation of the DMET differential cross sections is given elsewhere (Mansky 1990b). Data at other angles and energies are available upon request. As in the preceding paper, our discussion of the DCS results will be restricted to the forward direction ($\theta \leq 40°$). Due to the neglect of full polarization distortion and electron exchange the DMET results for the elastic $\sigma_{1^1S\rightarrow 1^1S}(\theta)$ are only in agreement with the experimental data of Jansen *et al* (1976) at high energies as expected.

The DMET DCS results for the excitation of the 2^1S and 2^1P states of He are in excellent agreement with the experimental data of Dillon and Lassettre (1975) for $E = 200$, 300, 400, 500 and 700 eV (only the data at 200 and 500 eV are shown in figures 3(*b*) and (*c*)). At lower energies, reasonable agreement is achieved between the DMET DCS (at 40 eV) for the 2^1S state and the experimental data of Hall *et al* (1973) (at 39.2 eV) and Trajmar (1973) (at 40.1 eV) for $\theta \leq 20°$. However, the DMET results underestimate both the position and depth of the diffraction-like minimum at $\theta = 50°$ observed in the data of Hall *et al* and Trajmar previously cited. It would appear that the DMET DCS results for the 2^1S state at 40 eV yield only a very shallow minimum at $\theta = 35°$, while the experimental data indicate that a great deal of destructive interference between the direct and exchange channels occurs, resulting in a much deeper minimum at larger scattering angles. In contrast, the FOMBT DCS results of Thomas *et al* (1974) correctly predict the position of the minimum in the 2^1S experimental data at both 29.6 and 40.1 eV (i.e. to within the angular resolution of the experimental

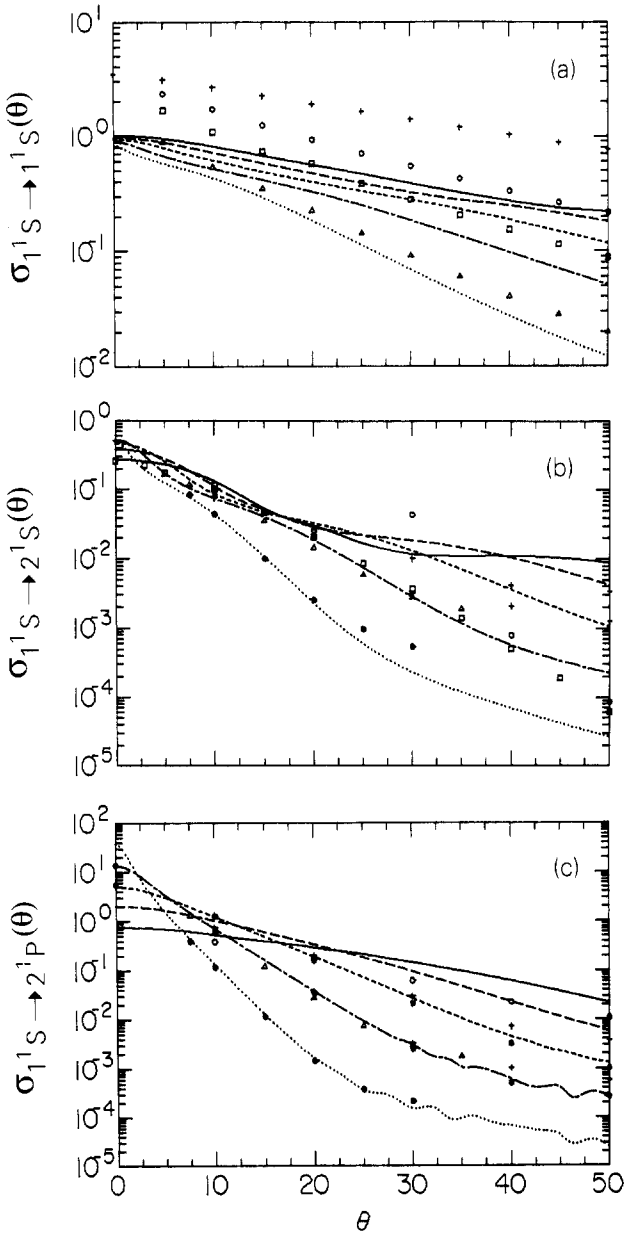

Figure 3. (*a*)-(*c*) Differential cross sections: (*a*) $\sigma_{1^1S\to1^1S}(\theta)$, (*b*) $\sigma_{1^1S\to2^1S}(\theta)$ and (*c*) $\sigma_{1^1S\to2^1P}(\theta)$ (all in a_0^2 sr^{-1}). Present DMET results for 40, 60, 100, 200 and 500 eV denoted by full curve, long broken curve, short broken curve, chain curve and dotted curve, respectively. In (*a*): +, McEachran and Stauffer (1983, E = 40 eV); ○, □, △, experimental data (Jansen 1975) for 100, 200 and 500 eV, respectively. In (*b*): +, Fon *et al* (1980) for 100, 200 eV; ○, experimental data (Hall *et al* 1973) at 39.2 eV; □, experimental data (Trajmar 1973) at 40.1 eV; △, ●, experimental data (Dillon and Lassettre 1975) at 200 and 500 eV, respectively. In (*c*): ⋆, DWPO (Scott and McDowell 1976) at 100 and 200 eV.

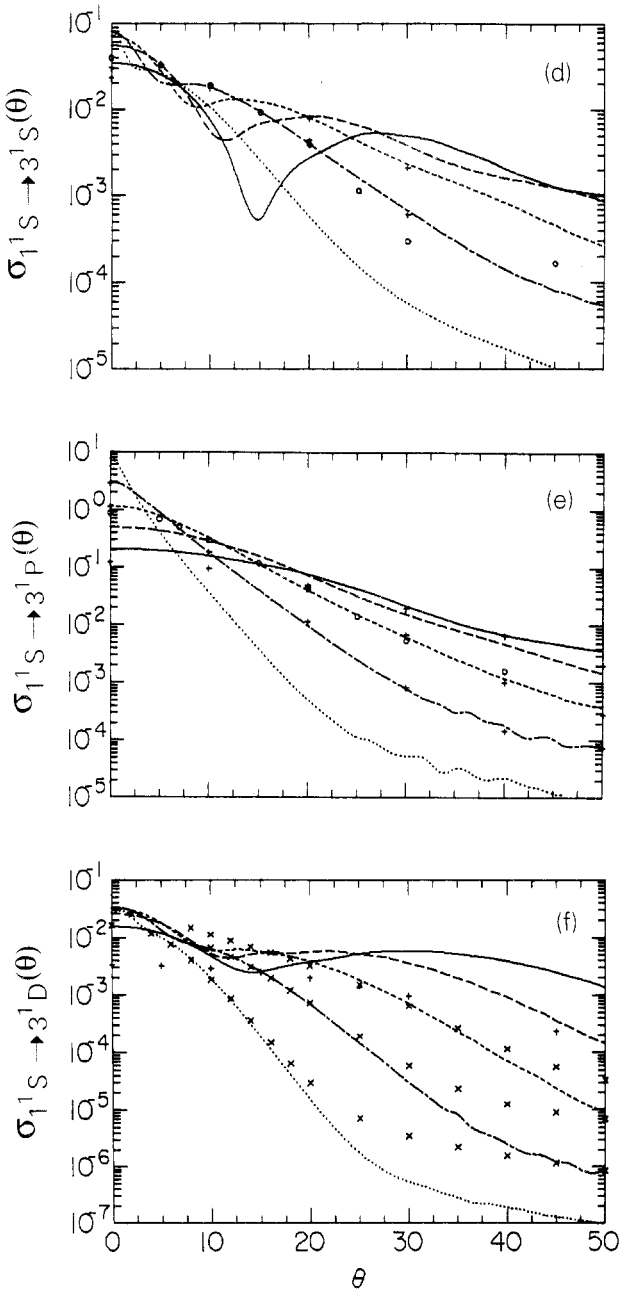

Figure 3. (*d*)-(*f*) Differential cross sections: (*d*) $\sigma_{1^1S\to3^1S}(\theta)$, (*e*) $\sigma_{1^1S\to3^1P}(\theta)$ and (*f*) $\sigma_{1^1S\to3^1D}(\theta)$ (all in a_0^2 sr^{-1}). All symbols are the same as figure 3(*a*)-(*c*) except where noted. In (*d*): +, DWPO (Scott and McDowell 1975) at 100, 200 eV; O, experimental data (Chutjian and Thomas 1975) at 39.7 eV. In (*e*): +, DWPO-I (Scott 1976) at 39.7, 100 and 200 eV; O, experimental data (Chutjian 1976) at 100 eV. In (*f*): +, FOMBT (Chutjian and Thomas 1975) at 39.7 eV; ×, Winters *et al* (1977) at 100, 200 and 500 eV.

data). But the FOMBT results of Thomas *et al* first overestimate, then underestimate the depth of the minimum in the data of Hall *et al* and Trajmar for the $\sigma_{1^1S\rightarrow 2^1S}(\theta)$ at 29.6 and 40.1 eV, respectively. The FOMBT results also underestimate the small angle ($\theta \leq 25°$) measurements at both energies. While the former discrepancy is not serious due to experimental uncertainty regarding the actual depth of the minimum (e.g. in Trajmar's experiment the width of the minimum in the 2^1S DCS at 29.6 and 40.1 eV was comparable with the angular resolution of the appartus), the latter discrepancy is due to an inadequate representation of the long range polarizability of the 2^1S state in the FOMBT. This difficulty can be corrected in distorted-wave theories by use of a suitable optical potential. However, this technique becomes difficult to implement when more than a few channels are included in the basis set. On the other hand, excellent agreement is obtained by the 19-state R-matrix DCS results of Fon *et al* (1988) with the measurements of Hall *et al* and Trajmar at 29.6 eV. It should also be noted that the DMET results and the 5-state R-matrix results of Fon *et al* (1980) for the $\sigma_{1^1S\rightarrow 2^1S}(\theta)$ are in good agreement for energies of 100 and 200 eV and scattering angles $\leq 30°$.

A more detailed comparison between the DMET results and other theoretical results for the $\sigma_{1^1S\rightarrow 2^1S}(\theta)$ is provided by tables 4 and 5 for E = 80–200 eV. These tables, together with table 3, replace tables 3.17 and 3.18 of Bransden and McDowell (1978), and clearly show that the DMET, and the original MET results of Flannery and McCann (1975a), are not an order of magnitude greater than other theoretical results, as concluded by Bransden and McDowell, but are of comparable magnitude. Also, the conclusion of Bransden and McDowell (1978, p 295) regarding the slow convergence of the 2^1S DCS at $\theta = 0°$ needs to be revised. In light of the results shown in table 5, it is apparent that convergence is essentially achieved when the strong $2^1S \rightarrow 2^1P_m$ dipole couplings are included in a calculation which solves the fully coupled set of equations appropriate to a given basis set. It is significant that the DMET and MET results differ from the 5-state R-matrix results (Fon *et al* 1980) at $\theta = 0°$ in tables 4(*b*) and 5 by only 6%, while all the other results in these tables fall significantly below (by factors from 2.4 to 4) the DMET and R-matrix results. Also, the R-matrix result in table 5 at 200 eV seems too high, while the impact parameter second-order potential (IPSOP) results of Berrington *et al* (1973) now seems anomalously large (compared with the other theoretical results).

In the case of the $1^1S \rightarrow 2^1P$ transition, the DMET DCS results are in relatively good agreement with the 39.2 eV measurements of Hall *et al* (1973), as well as with the theoretical results of the DWPO-I (Scott and McDowell 1976) and 5-state R-matrix (Fon *et al* 1980) at 100 and 200 eV (see figure 3(*c*)). A more detailed comparison is given in table 6 for the case of E = 80 eV. In that case the dipole corrections added in this paper to the MET DCS result in an increase of only 4% to $\sigma_{1^1S\rightarrow 2^1P}(\theta = 0°)$. At energies of 500 and 2000 eV the percentage increases to 18.7% and 54.7%, respectively. However, as the scattering angle θ increases from 0°, the relative contribution the dipole correction makes to the DMET $\sigma_{1^1S\rightarrow 2^1P}(\theta)$ declines dramatically—reaching the level of 1% or less for $\theta \geq 8°, 6°$ for E = 500, 2000 eV, respectively. This angular behaviour was expected and is a result of the large energy separation between the 1^1S and 2^1P states. The DMET DCS results for the 3^1S state are in agreement with the experimental data of Chutjian and Thomas (1975) only at small angles, and underestimate the position and depth of the diffractive-like minimum at larger angles. We also note that the DMET results are in good agreement with the DWPO-I

Table 3. DMET differential cross sections $\sigma_{1^1S\to 2^1S}(\theta)$ (a_0^2 sr^{-1}).

	E (eV)				
θ (deg)	40	60	100	200	500
0	2.71, −1	3.81, −1	4.72, −1	5.21, −1	4.93, −1
2	2.65, −1	3.62, −1	4.24, −1	4.00, −1	2.63, −1
4	2.44, −1	3.10, −1	3.12, −1	2.25, −1	1.51, −1
6	2.13, −1	2.39, −1	2.00, −1	1.36, −1	1.04, −1
8	1.74, −1	1.68, −1	1.26, −1	9.71, −2	6.99, −2
10	1.33, −1	1.11, −1	8.73, −2	7.50, −2	4.40, −2
12	9.43, −2	7.68, −2	6.66, −2	5.91, −2	2.59, −2
14	6.47, −2	5.82, −2	5.26, −2	4.65, −2	1.45, −2
16	4.63, −2	4.58, −2	4.37, −2	3.54, −2	7.90, −3
18	3.66, −2	3.54, −2	3.80, −2	2.63, −2	4.25, −3
20	3.04, −2	2.89, −2	3.30, −2	1.89, −2	2.30, −3
25	1.70, −2	2.21, −2	2.23, −2	7.50, −3	5.95, −4
30	1.19, −2	1.87, −2	1.33, −2	2.83, −3	2.28, −4
35	1.12, −2	1.48, −2	7.11, −3	1.16, −3	1.18, −4
40	1.12, −2	1.05, −2	3.62, −3	5.67, −4	6.89, −4

results of Scott and McDowell (1975) for $10° \leq \theta \leq 30°$ (see figure 3(d) and table 7). At $\theta = 0°$ the effects of polarization distortion are more pronounced as can be seen in table 7, wherein the DMET results are compared with the original MET (Flannery and McCann 1975a) and DWPO results (Scott and McDowell 1975). The latter both without (DWPO-I) and with (DWPO-II) polarization distortion in the direct channel. The good agreement between the DMET 3^1S DCS results and the extrapolated experimental data point of Chutjian and Thomas (at $\theta = 0°$) for $E = 39.7$ eV, when compared with the differences between the DMET and DWPO-II, again highlights the difficulty experienced by uncoupled representations in computing accurate DCS for optically forbidden transitions in the forward direction—especially for $E \leq 50$ eV. Note that table 7 replaces table 3.20 of Bransden and McDowell (1978, p 297).

At present no experimental data for $\sigma_{1^1S\to 3^1D}(\theta)$ exist. Also, because the 3^1D and 3^3D states of He are so close to the 3^1P state (13 and 14 meV separation, respectively), the two sets of experimental data available on the 3^1P DCS rely upon certain assumptions regarding the importance of the $3^{1,3}D$ states in the composite signal so that a signal due solely to the excitation of the 3^1P state can be identified. Hence, before discussing the DMET DCS results for 3^1P, we will discuss the $\sigma_{1^1S\to 3^1D}(\theta)$ theoretical results.

The DMET DCS results (figure 3(f)) for the 3^1D state are in good agreement with the impact parameter second-order potential distorted-wave (SOPDW) results of Winters *et al* (1977) at small scattering angles for energies $E = 100$, 200 and 500 eV. This is not suprising since both theories employ a semiclassical impact parameter representation without electron exchange to solve a set of coupled PDEs. The main difference between the DMET and SOPDW results lies in the details of the solution of the coupled equations in the two theories. This is the cause of the differences observed in figure 3(f) between the two theories at large scattering angles. On the other hand, the FOMBT results of Chutjian and Thomas (1975) at 39.7 eV are well below the DMET DCS result at 40 eV. This was expected since the FOMBT results of Chutjian

Table 4. (*a*) DMET Differential cross sections $\sigma_{1^1S\to2^1S}(\theta)$ (a_0^2 sr^{-1}). (*b*) Comparison of theoretical results for $\sigma_{1^1S\to2^1S}(\theta)$ (a_0^2 sr^{-1}).

(*a*)

	E (eV)		
θ (deg)	150	300	400
0	5.13, −1	5.21, −1	5.04, −1
10	7.90, −2	6.57, −2	5.45, −2
20	2.70, −2	8.75, −3	4.30, −3
30	5.94, −3	9.04, −4	4.07, −4
40	1.20, −3	2.21, −4	1.16, −4
50	4.10, −4	9.37, −5	4.67, −5
60	2.09, −4	4.44, −5	2.13, −5

(*b*)

θ (deg)	DMET[a]	DMET[b]	DMET[c]	MET[d]	DWPO-I[e]	FOMBT[f]	SOPDW[g]	R-matrix(5)[h]
0	4.43, −1	4.46, −1	4.46, −1	4.28, −1	1.08, −1	1.1, −1	1.18, −1	4.76, −1
10	9.54, −2	9.47, −2	9.45, −2	9.72, −2	8.17, −2†	8.5, −2	8.94, −2	1.29, −1
20	3.22, −2	3.24, −2	3.24, −2	2.96, −2	3.69, −2	3.9, −2	4.14, −2	3.06, −2
30	1.72, −2	1.70, −2	1.69, −2	1.77, −2	1.04, −2	1.2, −2	1.41, −2	1.21, −2
40	6.24, −3	6.04, −3	5.96, −3	6.41, −3	1.70, −3	4.0, −3		5.39, −3
50	1.91, −3	1.84, −3	1.81, −3	1.96, −3	1.74, −4	2.5, −3		4.53, −3
60	7.65, −4	7.32, −4	7.20, −4	7.61, −4	3.23, −4	2.5, −3	3.35, −3	4.78, −3

[a] Present results, $E = 80.00$ eV.
[b] Present results, $E = 81.20$ eV.
[c] Present results, $E = 81.63$ eV.
[d] Original results (Flannery and McCann 1975a), $E = 80.00$ eV.
[e] Distorted-wave polarized-orbital theory (Scott 1976, Table 11(*c*)), $E = 81.63$ eV.
[f] First-order many-body theory (Thomas *et al* 1974), $E = 81.63$ eV.
[g] Second-order potential distorted-wave theory (Bransden and Winters 1975), $E = 81.63$ eV.
[h] Five-state R-matrix theory (Fon *et al* 1980), $E = 81.63$ eV.
† Note that this value differs from that given in table 3.17(*b*) of Bransden and McDowell (1978). Here we have used the values given in Scott's thesis (1976).

Table 5. Comparison of theoretical results for $\sigma_{1^1S\to2^1S}(\theta = 0°)$ (a_0^2 sr^{-1}).

E (eV)	DMET[a]	MET[b]	DWPO-II[c]	EDW[d]	SOPDW[e]	FOMBT[f]	IPSOP[g]	R-matrix(5)[h]
100	4.72, −1	4.46, −1	2.00, −1	1.1, −1	1.3, −1	1.2, −1	1.50	5.00, −1
200	5.21, −1	5.00, −1	2.96, −1	1.6, −1			1.71	1.09

[a] Present results.
[b] Original results (Flannery and McCann 1975a).
[c] Distorted-wave polarized-orbital theory (Scott 1976, Table 11(*d*) and (*e*)).
[d] Eikonal distorted-wave theory (Joachain and Vanderpoorten 1974).
[e] Second-order potential distorted-wave theory (Bransden and Winters 1975).
[f] First-order many-body theory (Thomas *et al* 1974).
[g] Impact parameter second-order potential theory (Berrington *et al* 1973).
[h] Five-state R-matrix theory (Fon *et al* 1980).

Table 6. Comparison of theoretical results for $\sigma_{1^1S\rightarrow 2^1P}(\theta)$ (a_0^2 sr^{-1}).

θ (deg)	DMET[a]	DMET[b]	MET[c]	MET[d]	DWPO-I[e]	FOMBT[f]	R-matrix(5)[g]	Expt[h]
0	3.55	3.65	3.41	2.75	3.93	3.2	3.83	
10	1.24	1.24	1.24	1.30	1.28	1.15	1.37	9.64, −1
20	2.67, −1	2.61, −1	2.68, −1	2.53, −1	2.20, −1	5.71, −1	2.82, −1	1.54, −1
30	4.97, −2	4.72, −2	4.97, −2	4.95, −2	3.49, −2	3.30, −2	5.19, −2	3.00, −2
40	9.11, −3	8.52, −3	9.11, −3	9.25, −3	5.71, −3	6.70, −3	1.23, −2	1.00, −2
50	2.45, −3	2.29, −3	2.45, −3	2.36, −3	1.54, −3	2.87, −3	6.02, −3	5.00, −3
60	9.89, −4	9.51, −4	9.89, −4	8.98, −4	9.26, −4	2.08, −3	4.33, −3	3.39, −3

[a] Present results with dipole correction, E = 80.00 eV.
[b] Present results with dipole corretion, E = 81.63 eV.
[c] Present results without dipole correction, E = 80.00 eV.
[d] Original results without dipole correction (Flannery and McCann 1975a), E = 80.00 eV.
[e] Distorted-wave polarized-orbital theory (Scott and McDowell 1976), E = 81.63 eV.
[f] First-order many-body theory (Thomas *et al* 1974), E = 81.63 eV.
[g] Five-state R-matrix theory (Fon *et al* 1980), E = 81.63 eV.
[h] Experimental data (Chutjian and Srivastava 1975), E = 80 eV.

Table 7. Comparison of theoretical results for $\sigma_{1^1S\rightarrow 3^1S}(\theta)$ (a_0^2 sr^{-1}).

θ (deg)	DMET[a]	MET[b]	DWPO-I[c]	DWPO-II[d]
(*a*) 100 eV				
0	7.10, −2	7.26, −2	2.30, −2	3.79, −2
10	1.15, −2	1.43, −2	1.76, −2	2.06, −2
20	8.06, −3	6.87, −3	7.90, −3	6.02, −2
30	2.35, −3	1.83, −3	2.13, −3	1.24, −3
60	1.03, −4	8.43, −5	7.26, −5	6.54, −5
90	2.97, −5	2.29, −5	1.11, −4	8.84, −5
(*b*) 200 eV				
0	7.84, −2	7.77, −2	3.03, −2	5.71, −2
10	1.79, −2	1.81, −2	1.83, −2	1.80, −2
20	3.99, −3	3.50, −3	4.39, −3	2.92, −3
30	6.72, −4	5.44, −4	6.05, −4	3.91, −4
60	2.78, −5	2.39, −5	3.52, −5	2.82, −5
90	6.87, −6	4.98, −6	1.79, −5	1.42, −5

[a] Present results.
[b] Original results (Flannery and McCann 1975a).
[c] Distorted-wave polarized-orbital theory (Scott and McDowell 1975).
[d] Distorted-wave polarized-orbital theory (Scott 1976, table 13(*b*)).

and Thomas for $\sigma_{1^1S\rightarrow 3^1D}$ fall significantly below the Born, and are completely opposite the trend seen by experiment (see section 3.1). In fact, more recent FOMBT calculations by Cartwright and Csanak (1987), employing more accurate self-consistent wavefunctions for He, predict a 3^1D DCS result *below* that of Chutjian and Thomas.

Turning to the 3^1P state, the first set of measurements made of the 3^1P DCS (Chutjian and Thomas 1975) involved measuring the composite $\sigma_{1^1S\rightarrow 3^1P+3^1D+3^3D}(\theta)$ relative to the $\sigma_{1^1S\rightarrow 2^{1,3}P}(\theta)$. Chutjian and Thomas then placed their relative DCS measurements on an absolute scale by using the experimental data of Trajmar (1973) and Truhlar *et al* (1973) for the $2^{1,3}$P states. The resultant absolute experimental data

of Chutjian and Thomas for $\sigma_{1^1S\rightarrow 3^1P+3^1D+3^3D}(\theta)$ are shown in figure 4 for energies of 29.2 and 39.7 eV. The DMET results in figure 4 for the composite DCS underestimate the measurements of Chutjian and Thomas, while their FOMBT results are in good agreement with the experimental data they reported. However, since the FOMBT results underestimate the $\sigma_{1^1S\rightarrow 3^1D}$ integral cross section measurements for $E \leq 40$ eV, the possibility that a cancellation of errors in the FOMBT DCS results for the 3^1P and 3^1D states cannot be dismissed.

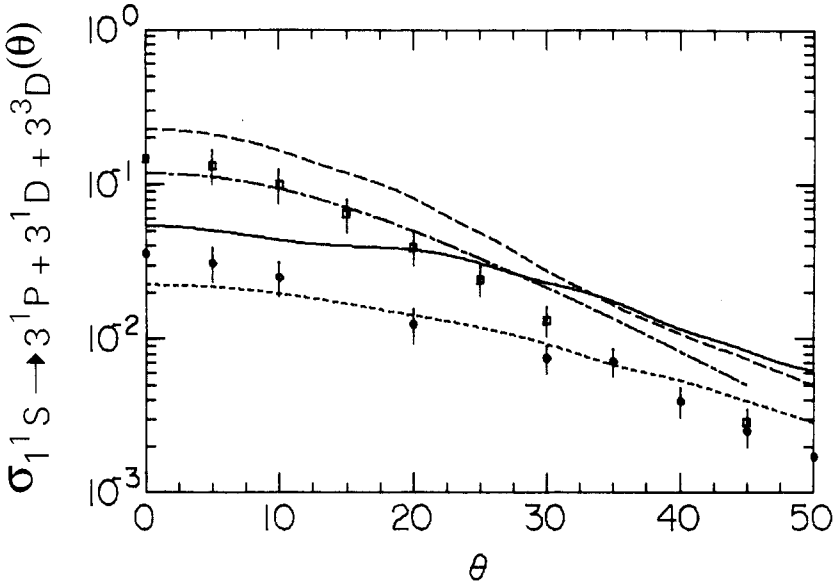

Figure 4. Differential cross section $\sigma_{1^1S\rightarrow 3^1P+3^1D+3^3D}(\theta)$ in a_0^2 sr^{-1}. Present DMET results at 29 and 40 eV are given by a full curve and long broken curve, respectively. FOMBT results (Chutjian and Thomas 1975) at 29.2 and 39.7 eV are given by a short broken curve and chain curve, respectively. O, □, experimental data (Chutjian and Thomas 1975) at 29.2 and 39.7 eV, respectively.

In the second set of measurements of the 3^1P DCS (Chutjian 1976), the composite $\sigma_{1^1S\rightarrow 3^1P+3^1D+3^3D}(\theta)$ was measured relative to the elastic DCS. After placing the results on an absolute scale (see Chutjian 1976 for details), a DCS, due solely to the $1^1S \rightarrow 3^1P$ transition, was isolated from the composite signal by eliminating the contribution from the $1^1S \rightarrow 3^{1,3}D$ channels. The contribution of the 3^3D state to the composite DCS was assumed by Chutjian to be negligible in the energy range 80–100 eV. This was inferred from the integral cross section measurements of Moussa *et al* (1969) where the $\sigma_{1^1S\rightarrow 3^3D}$ was only 1% of the $\sigma_{1^1S\rightarrow 3^1P}$ integral cross section for $E \leq 2$ keV. To subtract the contribution the 3^1D state made to the composite DCS, Chutjian used the original MET DCS results (Flannery and McCann 1975a) for the 3^1D state, renormalized (at small scattering angles) to reproduce the integral cross section results of Moussa *et al*, and assumed that the 3^1D state made only a negligible contribution to the composite DCS at large scattering angles. Chutjian based the latter assumption on the original FOMBT results (Chutjian and Thomas 1975) for the ratio $\sigma_{1^1S\rightarrow 3^1D}(\theta)/\sigma_{1^1S\rightarrow 3^1P}(\theta)$ which, at $E = 39.7$ eV, is ≤ 0.15 for $\theta \geq 100°$. The absolute 3^1P DCS finally determined by Chutjian (1976) is shown in figure 3(*e*) (for

$E = 100$ eV). Good agreement is obtained with the DMET results for $\theta \leq 40°$.

However, in an important experiment, van Linden van den Heuvell *et al* (1983) measured for the first time the orientation and alignment parameters characterizing the 3^1D state of He, and the ratio $\sigma_{1^1S\to3^1D}(\theta)/\sigma_{1^1S\to3^1P}(\theta)$ against E at $\theta = 35°$. They found the DCS ratio varied with energy—reaching a maximum value of 0.48 at 31.20 eV. In contrast, Chutjian (1976) assumed that the trends observed in the original FOMBT results for the DCS ratio at 39.7 eV would also hold in the energy range 80–100 eV. While the method of data reduction used by Chutjian for the 3^1P state made the best use of the limited theoretical and experimental data available at the time on the 3^1D DCS, the results of van Linden van den Heuvell *et al* indicate, however, that the contribution the 3^1D state makes to the composite DCS is not negligible, relative to the 3^1P DCS, and that it varies strongly with E. More detailed measurements of the 3^1P and 3^1D differential cross sections would be desirable.

A more quantitative view of the DMET 3^1P DCS results is given in table 8. Overall, the trend exhibited by the dipole correction to the 3^1P state is quite similiar to that observed earlier with the 2^1P state. That is, as the energy increases so does the relative importance of the dipole correction—eventually resulting in a 43% increase in the 3^1P DCS at $\theta = 0°$ and $E = 2$ keV.

Table 8. Comparison of theoretical results for $\sigma_{1^1S\to3^1P}(\theta)$ (a_0^2 sr^{-1}).

θ (deg)	DMET[a]	MET[b]	MET[c]	DWPO-I[d]	Expt[e]
0	7.93, −1	7.75, −1	7.273, −1	7.856, −1	(5.714, −1)†
5	6.29, −1	6.30, −1		5.714, −1	(4.285, −1)†
7	5.08, −1	5.12, −1			3.285, −1
10	3.32, −1	3.32, −1	3.645, −1	3.000, −1	2.214, −1
15	1.42, −1	1.41, −1		1.393, −1	9.999, −2
20	5.50, −2	5.50, −2	3.828, −2	6.071, −2	3.928, −2
25	2.25, −2	2.25, −2	1.555, −2	2.678, −2	1.678, −2
30	1.01, −2	1.01, −2	6.029, −3	1.107, −2	8.570, −3
35	4.75, −3	4.75, −3	2.580, −3		
40	2.29, −3	2.29, −3	1.246, −3	1.928, −3	3.214, −3

[a] Present results with dipole correction, $E = 80.00$ eV.
[b] Present results without dipole corretion, $E = 80.00$ eV.
[c] Original results (Flannery and McCann 1975a), $E = 80.00$ eV.
[d] Distorted-wave polarized-orbital theory (Scott and McDowell 1976 and private communication to Chutjian 1976), $E = 80.00$ eV.
[e] Experimental data (Chutjian 1976), $E = 80.00$ eV.
† Extrapolated results.

Before concluding our discussion of the DCS results, we compare in figure 5 the DMET results for the 2^1P_m DCS with the experimental data of Chutjian and Srivastava (1975) at 60 and 80 eV. Denote the DCS $\sigma_{1^1S\to n^1P_m}(\theta)$ by $\sigma_m(\theta)$ ($m = 0, 1$ and $n = 2, 3$). In figure 6 the DMET 3^1P_m DCS results are compared with the experimental data of Chutjian (1976) at 80 and 100 eV. In both sets of experimental data the magnetic substate differential cross sections were deduced using the λ parameters for the 2^1P and 3^1P states as measured by Eminyan *et al* (1974, 1975), respectively. Two general conclusions can be drawn from figures 5 and 6. First, the DMET results for the $\sigma_0(\theta)$ are in reasonable agreement with experimental data at small angles, while the DMET results for $\sigma_1(\theta)$ significantly overestimate the measured values in both figures. The DMET DCS $\sigma_1(\theta)$ results overestimate the experimental data presumably

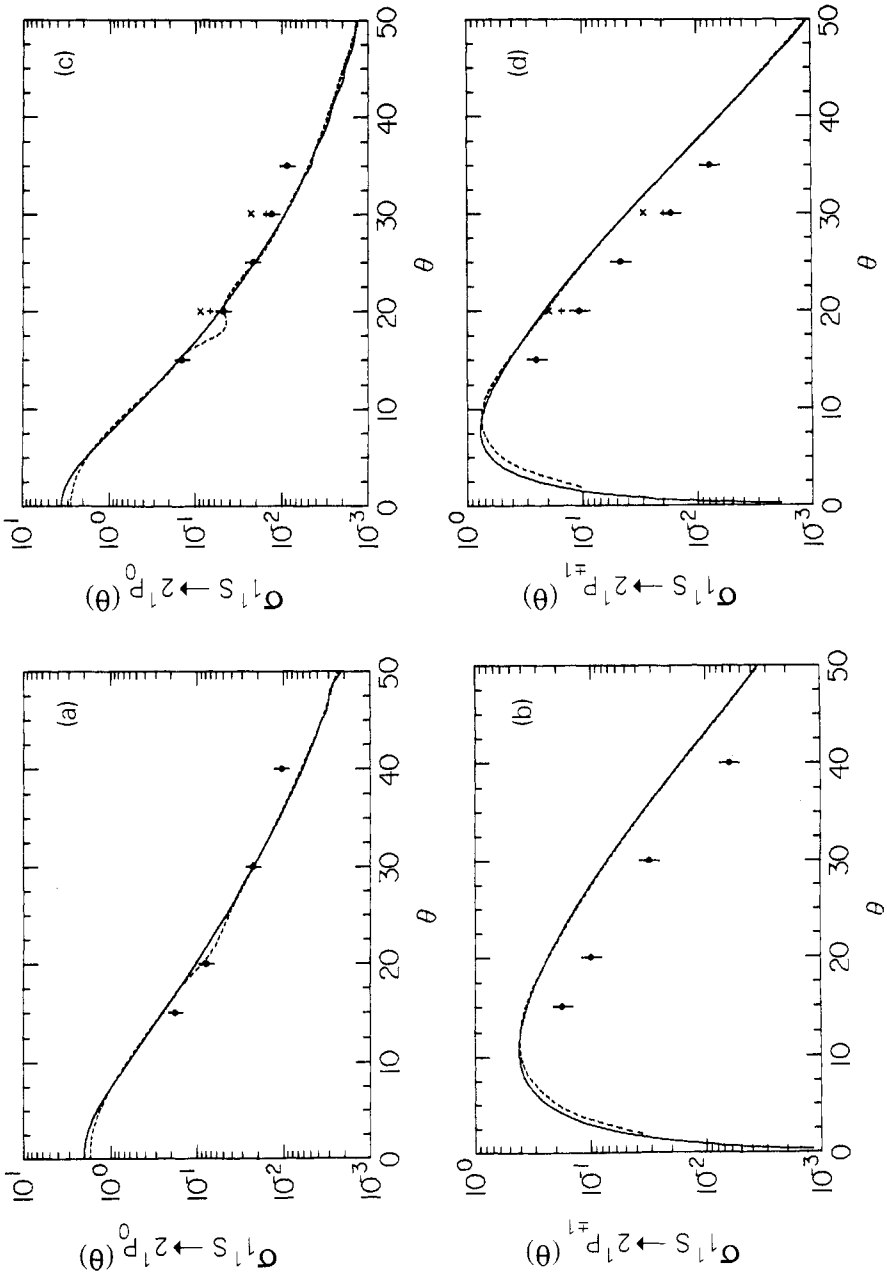

Figure 5. Magnetic sublevel differential cross sections $\sigma_{1^1S\rightarrow 2^1P_m}(\theta)$ (in a_0^2 sr^{-1}) (*a*) 2^1P_0, $E = 60$ eV, (*b*) $2^1P_{\pm 1}$, $E = 60$ eV, (*c*) 2^1P_0, $E = 80$ eV, (*d*) $2^1P\pm1$, $E = 80$ eV. Full curve, present DMET results; short broken curve, original MET results (Flannery and McCann 1975*a*); ×, 5-state *R*-matrix (Fon *et al* 1980) at 81.63 eV; +, DWPO-II (Scott and McDowell 1976); O, experimental data (Chutjian and Srivastava 1975).

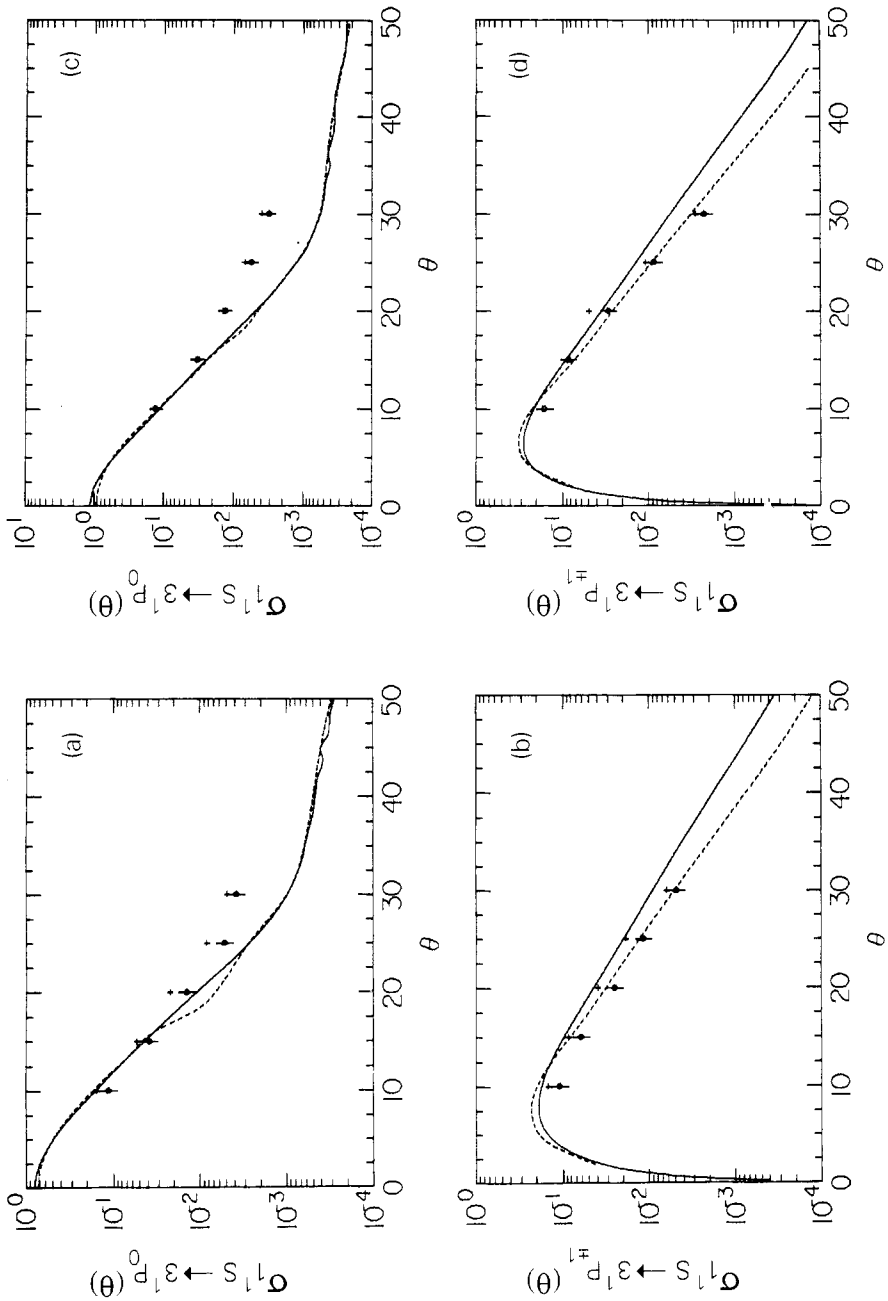

Figure 6. Magnetic sublevel differential cross sections $\sigma_{1^1S\rightarrow 3^1P_m}(\theta)$ (in a_0^2 sr^{-1}) (*a*) 3^1P_0, $E = 80$ eV, (*b*) $3^1P_{\pm 1}$, $E = 80$ eV, (*c*) 3^1P_0, $E = 100$ eV, (*d*) $3^1P_{\pm 1}$, $E = 100$ eV. Full curve, present DMET results; short broken curve, original MET results (Flannery and McCann 1975a); +, DWPO-II (Scott and McDowell 1976); O, experimental data (Chutjian 1976).

due to the neglect of electron exchange in the calculation—particularly the omission of transitions between the singlet and triplet manifolds which involve a change of magnetic quantum number of one or more ($\Delta \geq 1$).

The second main conclusion drawn from figures 5 and 6 is that the original MET results for $\sigma_0(\theta)$ at $\theta = 20°$ are incorrect (see figures 5(*c*) and 6(*a*)). The differences between the DMET and the original MET at this angle are a consequence of the improved numerical solution of the coupled equations (Mansky 1990a). Another consequence of the improved numerics is that the agreement between the original MET and experiment for the $\sigma_1(\theta)$ DCS at 80 and 100 eV (Chutjian 1976) is now seen to be fortuitous. The corresponding DMET results are seen to be consistent in their overestimation of the measured values of $\sigma_1(\theta)$ for the 2^1P and 3^1P states.

3.3. Polarization properties

Here we will concentrate on discussing the λ and χ parameters for the 2^1P and 3^1P states at an energy of 80 eV. A more detailed treatment of the orientation and alignment parameters for the 2^1P, 3^1P and 3^1D states of He will be given separately (Mansky 1990b), while the Stokes parameters for the 3^1D state are discussed in Mansky (1990c).

In figure 7 the DMET results for the λ and χ parameters for the 2^1P state are compared with the experimental data of Eminyan *et al* (1974) and Hollywood *et al* (1979) for $E = 80$ and 81.2 eV, respectively. The corresponding DMET results for the 3^1P state are shown in figure 8, together with the experimental data of Eminyan *et al* (1975) and Crowe *et al* (1981) for $E = 80$ and 75.6 eV, respectively. In both cases the DMET overestimates both the position and depth of the first minimum in the λ parameter at small angles. However, the DMET results in figures 7(*a*) and 8(*a*) clearly show that the oscillations in the original MET data at $\theta = 20°$ is incorrect, and is due to errors in the MET results for the $\sigma_1(\theta)$ (see section 3.2). Also, it is interesting to note the closeness of the DMET results and the 5-state R-matrix results (Fon *et al* 1980) for the λ and χ parameters at small angles. At larger angles ($\theta \geq 30°$), the differences between the two calculations are due primarily to electron exchange. In contrast, the differences between the DMET and DWPO-I results (Scott and McDowell 1976) at small angles is due to the inclusion in the DMET of the strong, long-range $2^1S \rightarrow 2^1P$, $3^1S \rightarrow 3^1P$, etc dipole couplings in the solution of the coupled equations. The fact that the DMET results are in quantitative agreement with the experimental data for the λ parameters in figures 7 and 8 only for $\theta \leq 20°$ is not suprising in view of the DMET results for the $\sigma_m(\theta)$ discussed in section 3.2. However, *no* theoretical results are at present in complete quantitative accord with the experimental data for the λ and χ parameters for the 2^1P and 3^1P states and energies in the range 50–500 eV. In fact, only near threshold are theory and experiment (Berrington *et al* 1987, Crowe and Nogueira 1982, Crowe *et al* 1983) for the 2^1P λ and χ parameters in quantitative agreement for a wide range of scattering angles. Hence, we conclude that the accurate theoretical prediction of the λ and χ parameters for n^1P states, in the case when many channels are open, will require inclusion of couplings between the singlet and triplet manifolds, with $\Delta \geq 1$. That is, solution of the full set of coupled integro-differential equations will be required, with a careful account taken of electron exchange effects in both the *primary* ($i \rightarrow f$), and *secondary* ($i \rightarrow n \rightarrow f$ and $i \rightarrow n \rightarrow n' \rightarrow f$, etc) mechanisms for excitation of the final state f.

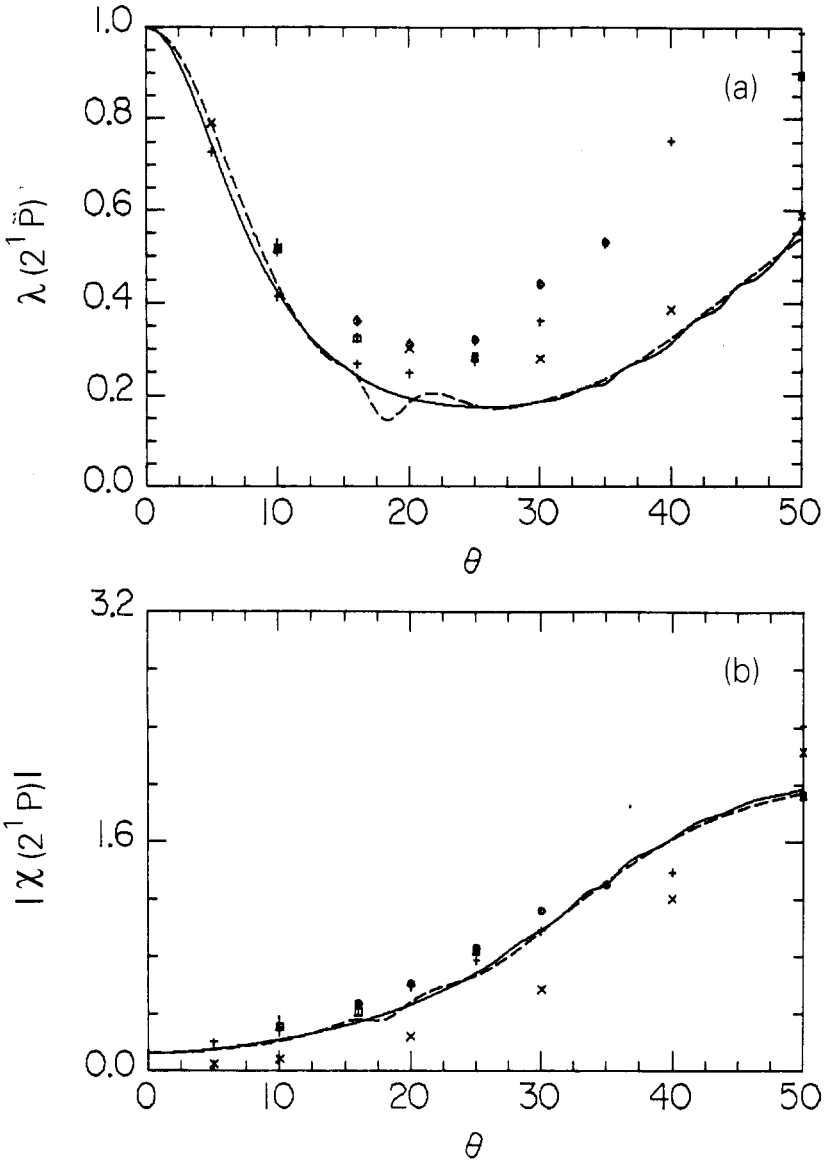

Figure 7. (*a*) λ, (*b*) $|\chi|$ (rad) parameters for the 2^1P state. Full curve, present DMET results at 81.20 eV; long broken curve, original MET results (Flannery and McCann 1975a) at 80 eV; +, 5-state *R*-matrix results (Fon *et al* 1980) at 81.63 eV; ×, DWPO-II (Scott and McDowell 1976) at 81.63 eV; ○, experimental data (Eminyan *et al* 1974) at 80 eV; □, experimental data (Hollywood *et al* 1979) at 81.20 eV.

4. Conclusions

The main conclusion of this paper is that the excitation of the 3^1S and 3^1D states occurs mainly via indirect couplings to one (or more) intermediate states. That is, more flux is tranferred to the $3^1S, 3^1D$ states, from the 1^1S state, by indirect mechanisms like $1^1S \rightarrow 2^1P \rightarrow 3^1S$, $1^1S \rightarrow 3^1P \rightarrow 3^1D$, etc than by the direct mechanisms $1^1S \rightarrow 3^1S$, $1^1S \rightarrow 3^1D$. While this result is well known, it has several consequences

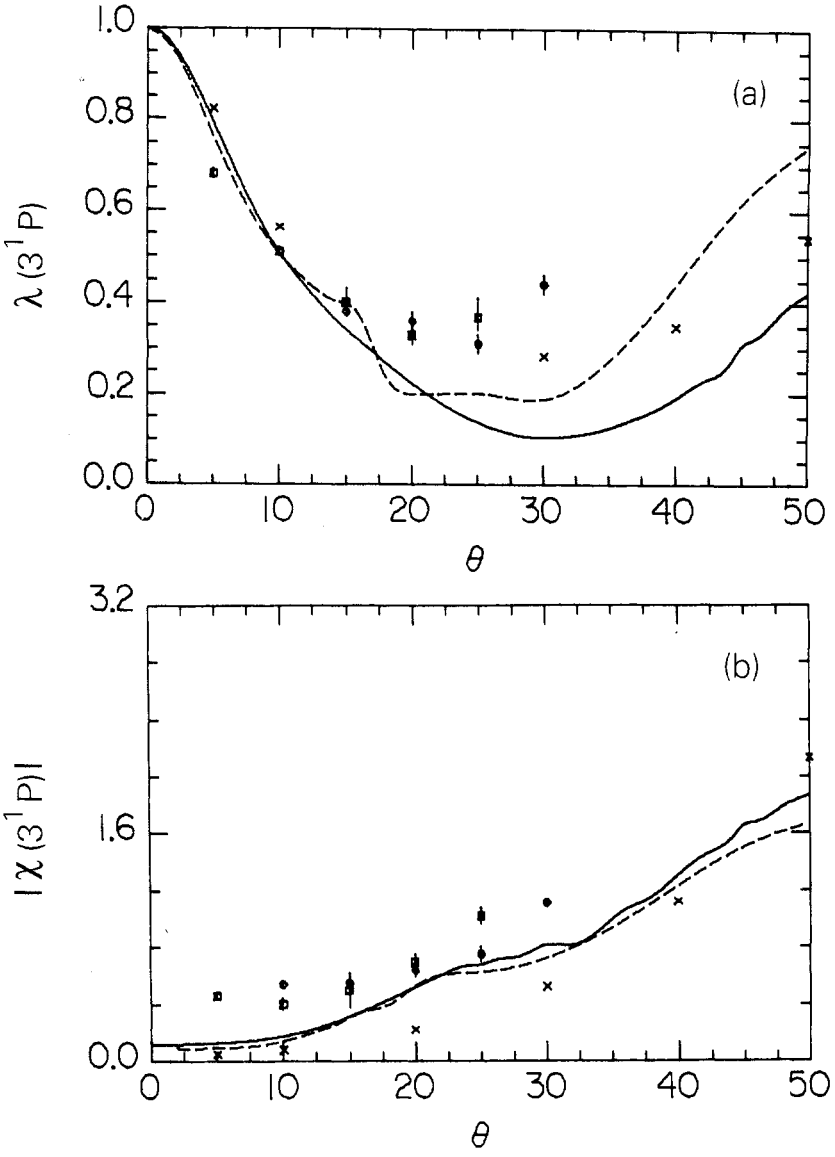

Figure 8. (*a*) λ, (*b*) $|\chi|$ (rad) parameters for the 3^1P state. Full curve, present DMET results at 75.60 eV; long broken curve, original MET results (Flannery and McCann 1975a) at 80 eV; ×, DWPO-II (Scott and McDowell 1976) at 80 eV; ○, experimental data (Eminyan *et al* 1975) at 80 eV; □, experimental data (Crowe *et al* 1981) at 75.60 eV.

which have not been recognized in the past. First is the interesting behaviour of the DMET $\sigma_{1^1S\to3^1S}$, $\sigma_{1^1S\to3^1D}$ integral cross sections (see figures 2(*c*) and (*e*)). While this behaviour has not been confirmed quantitatively by experiment, the overall consistent behaviour of the DMET results for the integral and DCS and the underlying orientation and alignment parameters (see section 3.3 and Mansky and Flannery 1987) argues strongly for their serious study. Also, more detailed measurements of the integral and differential cross sections for the 3^1L states of He at energies $E \leq 50$ eV would be

welcome.

The second consequence of the DMET results for the $n = 3$ states of He follows from comparing the R-matrix and distorted-wave results with the DMET results for the DCS and orientation and alignment parameters for the 3^1L states. Namely, that a careful analysis of the contribution that exchange-dominated transitions like $1^1S \rightarrow 2^3S \rightarrow 3^1P$, $1^1S \rightarrow 2^3P \rightarrow 3^1D$, etc make to the DCS and orientation and alignment parameters for the 3^1L states will be required in order to get good, quantitative agreement with experimental data over a wide range of scattering angles—especially in the intermediate energy region where many channels are open. An example of this is the $\sigma_{1^1S \rightarrow 3^1S}$ results in figure 2(c), where the 11-state R-matrix results (Berrington *et al* 1985) are nearly a factor of five larger than the DMET results at 29.2 eV. It is doubtful whether such an increase is due solely to inclusion of electron exchange in the transition $1^1S \rightarrow 3^1S$. Rather, inclusion of exchange-dominated dipole transitions like $1^1S \rightarrow 2^3P \rightarrow 3^1S$ within a full set of coupled equations will be required for the accurate prediction of integral cross sections for the excitation of the $n \geq 3$ states of He.

Acknowledgments

This research is supported by the US Air Force Office of Scientific Research under Grant No AFOSR-89-0426.

References

Anderson R J, Hughes R H and Norton T G 1969 *Phys. Rev.* **181** 198–205
Bashkin S and Stoner Jr J O 1975 *Atomic Energy Levels and Grotrian Diagrams, vol 1, Hydrogen I–Phosphorus XV* (Amsterdam: North-Holland)
Baye D and Heenen P-H 1974a *J. Phys. B: At. Mol. Phys.* **7** 928–37
—— 1974b *J. Phys. B: At. Mol. Phys.* **7** 938–49
Bell K L, Kennedy D J and Kingston A E 1969 *J. Phys. B: At. Mol. Phys.* **2** 26–43
Berrington K A, Bransden B H and Coleman J P 1973 *J. Phys. B: At. Mol. Phys.* **6** 436–49
Berrington K A, Burke P G, Freitas L C G and Kingston A E 1985 *J. Phys. B: At. Mol. Phys.* **18** 4135–47
Berrington K A, Burke V M, Burke P G and Scialla S 1989 *J. Phys. B: At. Mol. Opt. Phys.* **22** 665–76
Berrington K A, Fon W C, Freitas L C G and Kingston A E 1987 *J. Phys. B: At. Mol. Phys.* **20** L685–90
Berrington K A and Kingston A E 1987 *J. Phys. B: At. Mol. Phys.* **20** 6631–40
Bransden B H and Issa M R 1975 *J. Phys. B: At. Mol. Phys.* **8** 1088–94
Bransden B H and McDowell M R C 1978 *Phys. Rep.* **46** 249–394
Bransden B H and Winters K H 1975 *J. Phys. B: At. Mol. Phys.* **8** 1236–44
Cartwright D C and Csanak G 1987 *J. Phys. B: At. Mol. Phys.* **20** L583–90 (see also corrigendum in 1988 *J. Phys. B: At. Mol. Opt. Phys.* **21** 1717)
Chan F T and Chang C H 1975 *Phys. Rev.* A **12** 1383–92
Chung S and Lin C C 1968 *Bull. Am. Phys. Soc.* **13** 214
—— 1969 *Proc. 6th Int. Conf. on the Physics of Electronic and Atomic Collisions, Cambridge, MA* (Cambridge, MA: MIT Press) Abstracts pp 363–4
Chutjian A 1976 *J. Phys. B: At. Mol. Phys.* **9** 1749–56
Chutjian A and Srivastava S K 1975 *J. Phys. B: At. Mol. Phys.* **8** 2360–8
Chutjian A and Thomas L D 1975 *Phys. Rev.* A **11** 1583–95
Cohen M and McEachran R P 1967 *Proc. Phys. Soc.* **92** 37–41
Crothers D S F and McEachran R P 1970 *J. Phys. B: At. Mol. Phys.* **3** 976–90

Crowe A, King T C F and Williams J F 1981 *J. Phys. B: At. Mol. Phys.* **14** 1219–28
Crowe A and Nogueira J C 1982 *J. Phys. B: At. Mol. Phys.* **15** L501–5
Crowe A, Nogueira J C and Liew Y C 1983 *J. Phys. B: At. Mol. Phys.* **16** 481–9
de Heer F J and Jansen R H J 1977 *J. Phys. B: At. Mol. Phys.* **10** 3741–58
Dillon M A and Lassettre E N 1975 *J. Chem. Phys.* **62** 2373–90
Donaldson F G, Hender M A and McConkey J W 1972 *J. Phys. B: At. Mol. Phys.* **5** 1192–210
Donnelly B P and Crowe A 1988 *J. Phys. B: At. Mol. Phys.* **21** L637–43
Donnelly B P, Neill P A and Crowe A 1988 *J. Phys. B: At. Mol. Opt. Phys.* **21** L321–5
Eminyan M, MacAdam K B, Slevin J and Kleinpoppen H 1974 *J. Phys. B: At. Mol. Phys.* **7** 1519–42
Eminyan M, MacAdam K B, Slevin J, Standage M C and Kleinpoppen H 1975 *J. Phys. B: At. Mol. Phys.* **8** 2058–66
Feldman F R and MacAlpine G M 1978 *Astrophys. J.* **221** 486–500
Ferland G J 1986 *Astrophys. J.* **310** L67–70
Flannery M R and McCann K J 1975a *J. Phys. B: At. Mol. Phys.* **8** 1716–33
—— 1975b *Phys. Rev.* A **12** 846–55
Fon W C, Berrington K A, Burke P G and Kingston A E 1981 *J. Phys. B: At. Mol. Phys.* **14** 2921–34
Fon W C, Berrington K A and Kingston A E 1980 *J. Phys. B: At. Mol. Phys.* **13** 2309–25
—— 1988 *J. Phys. B: At. Mol. Opt. Phys.* **21** 2961–8
Hall R I, Joyez G, Mazeau J, Reinhardt J and Schermann C 1973 *J. Physique* **34** 827–43
Hollywood M T, Crowe A and Williams J F 1979 *J. Phys. B: At. Mol. Phys.* **12** 819–34
Jansen R H J 1975 *PhD Thesis* Amsterdam
Jansen R H J, de Heer F J, Luyken H J, van Wingerden B and Blaauw H J 1976 *J. Phys. B: At. Mol. Phys.* **9** 185–212
Joachain C J and Vanderpoorten R 1974 *J. Phys. B: At. Mol. Phys.* **7** 817–30
Kay R B and Simpson C G 1988 *J. Phys. B: At. Mol. Opt. Phys.* **21** 625–37
Mansky E J 1990a *J. Comput. Phys.* to be submitted
—— 1990b *J. Phys. B: At. Mol. Opt. Phys.* to be submitted
—— 1990c *Z. Phys.* D to be submitted
Mansky E J and Flannery M R 1987 *J. Phys. B: At. Mol. Phys.* **20** L235–9
—— 1990 *J. Phys. B: At. Mol. Opt. Phys.* **23** 4549
Massey H S W, Burhop E H S and Gilbody H B 1969 *Electronic and Ionic Impact Phenomena* vol 1 (Oxford: Clarendon) pp 491–5
—— 1974 *Electronic and Ionic Impact Phenomena* vol 5 (Oxford: Clarendon) pp 3387-91
McCann K J and Flannery M R 1974 *Phys. Rev.* A **10** 2264–72
—— 1975 *J. Chem. Phys.* **63** 4695–4707
—— 1978 *J. Chem. Phys.* **69** 5275–87
McEachran R P 1974 private communication to M R Flannery
McEachran R P and Cohen M 1969 *J. Phys. B: At. Mol. Phys.* **2** 1271–3
McEachran R P and Stauffer A D 1983 *J. Phys. B: At. Mol. Phys.* **16** 255–74
Moussa H R M, de Heer F J and Schutten J 1969 *Physica* **40** 517–49
Müller-Fiedler R, Schlemmer P, Jung K, Hotop H and Ehrhardt H 1984 *J. Phys. B: At. Mol. Phys.* **17** 259–68
Rall D L A, Sharpton F A, Schulman M B, Anderson L W and Lin C C 1989 *Phys. Rev. Lett.* **62** 2253–6
Phelps A V 1955 *Phys. Rev.* **99** 1307–13
Scott T 1976 *PhD Thesis* London
Scott T and McDowell M R C 1975 *J. Phys. B: At. Mol. Phys.* **8** 1851–64
—— 1976 *J. Phys. B: At. Mol. Phys.* **9** 2235–54
Shemansky D E, Ajello J M, Hall D T and Franklin B 1985 *Astrophys. J.* **296** 774–83
Showalter J G and Kay R B 1975 *Phys. Rev.* A **11** 1899–910
St John R M, Miller F L and Lin C C 1964 *Phys. Rev.* **134** A888–97
Thomas L D, Csanak G, Taylor H S and Yarlagadda B S 1974 *J. Phys. B: At. Mol. Phys.* **7** 1719–33
Trajmar S 1973 *Phys. Rev.* A **8** 191–203
Truhlar D G, Trajmar S, Williams W, Ormonde S and Torres B 1973 *Phys. Rev.* A **8** 2475–82
van den Bos J, Winter G J and de Heer F J 1968 *Physica* **40** 357–84
van Linden van den Heuvell H B, van Gasteren E M, van Eck J and Heideman H G M 1983 *J. Phys. B: At. Mol. Phys.* **16** 1619–31
van Raan A F J, de Jongh J P, van Eck J and Heideman H G M 1971 *Physica* **53** 45–59

van Raan A F J, Moll P G and van Eck J 1974 *J. Phys. B: At. Mol. Phys.* **7** 950–65
van Raan A F J and van Eck J 1974 *J. Phys. B: At. Mol. Phys.* **7** 2003–20
van Zyl B, Dunn G H, Chamberlain G and Heddle D W O 1980 *Phys. Rev.* A **22** 1916–29
Vriens L 1967 *Phys. Rev.* **160** 100–8
Westerveld W B, Heideman H G M and van Eck J 1979 *J. Phys. B: At. Mol. Phys.* **12** 115–35
Willis S L, Hata J, McDowell M R C, Joachain C J and Byron Jr F W 1981 *J. Phys. B: At. Mol. Phys.* **14** 2687–704
Winters K H, Issa M and Bransden B.H 1977 *Can. J. Phys.* **55** 1074–82